UNIVERSIDAD DE SANTIAGO DE CHILE
FACULTAD DE CIENCIAS
Departamento de Física

Parametric Resonance effects in Dark Matter Production in Standard and Non-Standard Cosmology

Luciano Alejandro Venegas Millar

Profesora Guía: Paola Arias Reyes

Tesis para optar al grado académico de Magíster en Ciencia con Mención en Física.

Santiago - Chile

2023

Abstract

Up until today, Dark Matter is one of the most important problems yet to solve in physics and there are several approaches to try and learn more about its nature and general properties. We have focused our study on trying to delimit the parameter space that allows us to recreate the data obtained up until today. In this master's thesis, we consider a cosmological scenario different than the one presented by ΛCDM to explore different possibilities to explain the dark matter present in the universe in relation to its production mechanism and stability as well as its interactions with other particles, within the standard model or the hidden sector. We implemented a non-standard cosmology that considers the presence of an additional field responsible to dominate the energy density of the universe prior to primordial nucleosynthesis. We perform a detailed analysis of the effects of the presence of this field in relation to the expansion of the universe and the dark matter relic density for different scenarios and apply these effects to the known results of stability of dark matter candidates affected by resonant decay processes. We analyze the decay of dark matter candidates in exponentially efficient processes and define bounds that allow to explain the dark matter relic density on each model. We present results that can account for the total dark matter density present today for a wide parameter space of the coupling of the models and the mass of the dark matter candidates.

This manuscript is organized as follows, in the first chapter, we do an overview of cosmology and general concepts necessary for this work. Then, we present the dark matter candidates of interest and their production mechanisms. Also, we present the essentials of non-standard cosmology and implement it to compare it with the stipulated by ΛCDM to show the crucial differences in the expansion of the universe and the dark matter relic density for different cosmological scenarios. Finally, we implement these results on two different models for dark matter candidates and show the impact on the parameter space that allows to account for the dark matter energy density at the present day in several cosmological cases in comparison to the results obtained by ΛCDM.

Keywords: Cosmology, Dark Matter, Misalignment mechanism, Parametric resonance

Resumen

A día de hoy, la Materia Oscura es uno de los problemas más importantes en la física que se encuentra aún por resolver y existen múltiples ángulos para tratar de aprender más sobre su naturaleza y propiedades generales. Hemos centrado nuestro estudio en intentar delimitar el espacio de parámetros que nos permita recrear los datos obtenidos al día de hoy. En esta tesis de magíster, consideramos un escenario cosmológico diferente al presentado por ΛCDM para explorar diferentes posibilidades de explicar la materia oscura presente en el universo en relación a su mecanismo de producción y estabilidad así como sus interacciones con otras partículas, dentro del modelo estándar o en el sector oscuro. Implementamos una cosmología no estándar que considera la presencia de un campo adicional responsable de dominar la densidad de energía del universo previo a la nucleosíntesis primordial. Realizamos un análisis detallado de los efectos de la presencia de este campo en relación a la expansión del universo y la densidad de reliquia de la materia oscura para diferentes escenarios y aplicamos estos efectos a resultados conocidos respecto a estabilidad de candidatos a materia oscura afectados por procesos de decaimiento resonante. Analizamos el decaimiento de candidatos a materia oscura en procesos exponencialmente eficientes y definimos restricciones que permitan explicar la densidad de reliquia de materia oscura en cada modelo. Presentamos resultados que pueden dar cuenta del total de materia oscura presente hoy para un amplio espacio de parámetros de el acoplo de los modelos y la masa de los candidatos a materia oscura.

Este escrito está organizado de la siguiente manera, en el primer capítulo, realizamos una revisión de cosmología y conceptos generales necesarios para este trabajo. Luego, presentamos los candidatos a materia oscura de interés y sus mecanismos de producción. Además, presentamos los puntos esenciales de la cosmología no estándar y lo implementamos para compararlo con lo estipulado por ΛCDM para mostrar las diferencias cruciales en la expansión del universo y la densidad de reliquia de materia oscura para diferentes escenarios cosmológicos. Finalmente, implementamos estos resultados en dos modelos diferentes de candidatos a materia oscura y mostramos el impacto en el espacio de parámetros que permite dar cuenta de la densidad de materia oscura al día de hoy en diferentes casos, en comparación a los resultados obtenidos por ΛCDM

Palabras clave: Cosmología, Materia oscura, Resonancia paramétrica, Mecanismo de misalignment

Acknowledgements

I would like to express my gratitude to my advisor, Dr. Paola Arias, for her assistance and support throughout every step of the project, and for her patience and encouragement to reach further.

I would like to express my complete gratitude to ANID, for funding my Masters's degree study with the scholarship ANID-Subdirección de Capital Humano/ Magíster Nacional/ Año 2022 - 28122021.

Finally, I would also like to thank the Universidad de Santiago de Chile for the research support grants.

Thank you, Alex.

Agradecimientos

Quiero expresar mi gratitud a mi supervisora, la Profesora Paola Arias, por su apoyo, motivación y entusiasmo en el proceso, por la paciencia y la guía entregada en estos años.

Quiero agradecer a ANID por la Beca de Magíster Nacional año académico 2022 otorgada así como a la Universidad de Santiago de Chile por las becas y apoyo a la investigación.

Quiero agradecer a mi pareja Natalia por acompañarme y alentarme en cada paso, tu compañía ha hecho que este camino sea aún más hermoso. A mis amigos, Daniela, Sebastián, Ángel, Víctor, Fernanda, Ignacio, Cyntia, Ayrton, Moira y a todos quienes me ayudaron a llegar aquí.

Finalmente quiero agradecer a mi familia, esto es para ustedes, por su incondicional apoyo incluso en los momentos difíciles. Nada sería suficiente para retribuirles. Gracias por permitirme seguir mi camino.

Contents

List of Figures

Chapter 1

Introduction

The Standard Model of Particle Physics (SM) is one of the most successful theories developed in the last decades, with incredible precision and predictions related to how the universe works under three of the fundamental interactions, corresponding to electromagnetic, weak, and strong forces, but it is still an incomplete theory. The SM lacks a Dark Matter (DM) candidate who is stable, cold, and weakly coupled, it also does not provide a clear way to explain the matter-anti-matter asymmetry and the big structure formation [1, 2], among others. This motivates us to consider new physics beyond SM. In this chapter, we will take a look at the theoretical concepts that allow us to dive into the DM problem.

1.1 Dark Matter

The DM problem is one of the most important questions in modern cosmology. It is responsible for approximately 26% of the universe's energy density [3] but its nature is still unknown.

One of the first indicators of the existence of the DM came from astronomical observations related to the rotation curves of galaxies [4, 5]. It was shown that the predictions corresponding to the rotation velocity of galaxies produced by their baryonic matter were much smaller than the measurements, as we move away from their center. This, among other puzzling observations, lead to considering a matter component different from the ordinary baryonic mass in the form of a halo of nonluminous unknown matter, which was named Dark Matter. To explain the data, a galaxy's total matter must consist of more than 95% of DM, these results are shown if Fig. (1.1), where we can see that the DM consideration gives us a good fit to the data [6].

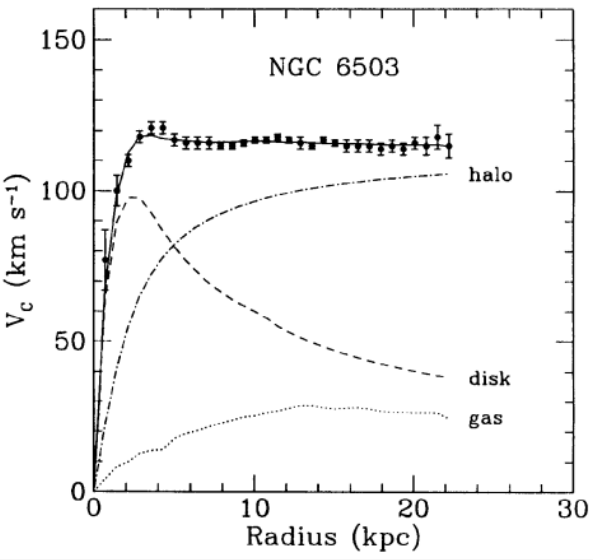

Figure 1.1: Data of the galactic rotation curve for NGC 6503 of the disk and gas contribution plus DM halo needed to fit the data (from [6]).

Measurements of the Cosmic Microwave Background (CMB) provide outstandingly precise values of several cosmological parameters and it also provides us with evidence for the existence of DM hidden in its temperature anisotropies. The CMB is the remnant radiation from recombination era where the first atoms were formed, therefore, contains information related to the early stages of the universe. As the plasma collapsed inwards by gravitational effects, the photon pressure created a resistance. This struggle between pressure and gravitation created a distinctive pattern of peaks in the CMB spectrum. The study of those temperature fluctuations allowed us to estimate the amount of gravitational matter present in the early universe, in fact, this alone provides enough evidence for the existence of DM [6].

Another way to confirm the existence of DM has been found in gravitational lensing, since gravitational effects of energy density alter the light patterns, the data obtained from galaxies clusters [7] require the existence of DM.

Besides the data that gives us reasons to study physics beyond SM, we have no certainty about the nature of DM although there has been found several conditions that must be fulfilled to consider a viable DM candidate.

In the next chapter, we will do a brief review of DM candidates and their important features related to this work.

1.2 Overview of Cosmology

Our current understanding of the evolution of the universe is based on the Friedman-Robertson-Walker (FRW) cosmological model. It is also known as Standard Cosmology or ΛCDM. Direct evidence supporting its validity extends back to the epoch called Big-Bang Nucleosynthesis, about 10^2 s after the Big-Bang. This model considers the matter and radiation distribution of the universe to be homogeneous and isotropic at large scales.

The metric for a space with homogeneous and isotropic spatial sections is the maximally-symmetric FRW metric, which can be written as

$$ds^2 = dt^2 - R^2(t)\left(\frac{dr^2}{1-kr^2} + r^2 d\theta^2 + r^2 \sin^2\theta d\phi^2\right) \tag{1.1}$$

where t is the physical time, $R(t)$ is the cosmic scale parameter and k is the spatial curvature constant.

To further analyze the dynamics of the expanding universe, it is necessary to look at the scale factor using Eintein's equations

$$R_{\mu\nu} - \frac{1}{2}\mathcal{R}g_{\mu\nu} \equiv G_{\mu\nu} = 8\pi G T_{\mu\nu} + \Lambda g_{\mu\nu}, \tag{1.2}$$

where $G_{\mu\nu}$ is the Einstein tensor, $T_{\mu\nu}$ is the stress-energy tensor, and Λ is the cosmological constant. If we look at Einstein's equations and the fact that the stress-energy tensor $T_{\mu\nu}$ takes into account all the fields present, we see that to be consistent with the symmetries of the metric, $T_{\mu\nu}$ must be diagonal, and by isotropy, all the spatial component must be equal. Let us then consider a perfect fluid characterized by $\rho(t)$ as its energy density and $p(t)$ its pressure, we obtain:

$$T^{\mu}{}_{\nu} = diag(\rho, -p, -p, -p). \tag{1.3}$$

Requiring the conservation of the stress energy-momentum tensor ($T^{\mu\nu}{}_{;\nu} = 0$) we obtain the continuity equation for the $\mu = 0$ component

$$d(\rho R^3) = -p d(R^3). \tag{1.4}$$

This allows us to obtain a simple relation between the energy density and the scale parameter. If we consider the simple equation of state for a perfect fluid, $p = \omega\rho$, we obtain

$$\rho \propto R^{-3(1+\omega)}. \tag{1.5}$$

Moreover, going back to the Einstein equations for the FWR metric we obtain the Friedmann equations.

$$H^2 + \frac{k}{R^2} = \frac{8\pi G}{3}\rho + \frac{\Lambda}{3}, \tag{1.6}$$

$$\frac{\ddot{R}}{R} = -\frac{4\pi G}{3}(\rho + 3p). \tag{1.7}$$

where we have introduced $H = \frac{\dot{R}}{R}$, called the Hubble parameter and Λ is associated to the dark energy density. Our study is focused on the early stages of the universe, thus we will set $\Lambda = 0$. Equations (1.6) and (1.7) describe the evolution of the universe for any given energy content. We can rearrange eq. (1.6) to express a few useful parameters by

$$\frac{k}{H^2R^2} = \frac{\rho}{3H^2/8\pi G} - 1 \equiv \Omega - 1 \tag{1.8}$$

where Ω is the density parameter defined as the ratio of the density to the critical density:

$$\Omega \equiv \frac{\rho}{\rho_C} \quad , \quad \rho_C = \frac{3H^2}{8\pi G}. \tag{1.9}$$

we see clearly that the sign of k depends on this ratio, e.g. for $\rho = \rho_C$ we obtain a flat universe.

It is important to notice that ρ and p are composed by all the fields' contributions so we obtain a density ratio for each field as well.

A few important parameters in the present universe are [3]

$$H_0 \approx 100h \text{ km s}^{-1} \text{ Mpc}^{-1}, \quad \rho_C \approx 3.44 \times 10^{-47} \text{ GeV}^{-4}. \tag{1.10}$$

and related to the density parameter for dark energy, radiation, and matter respectively

$$\Omega_{\Lambda,0} \approx 0.68, \tag{1.11}$$

$$\Omega_{r,0} \approx 10^{-5}, \tag{1.12}$$

$$\Omega_{b,0} \approx 0.04, \tag{1.13}$$

$$\Omega_{DM,0} \approx 0.26, \tag{1.14}$$

where b corresponds to the baryonic matter and the subindex 0 represents the value at the present time. It is important to mention that H_0 presents a very important challenge in modern physics due to the Hubble tension, which corresponds to the disagreement found between the estimations of considering ΛCDM and the measurements related to the luminosity distance and redshift of known standard candles[8, 9].

Due to the observational data, the universe is considered to be flat at large scales [1], then considering Eq. (1.6) we obtain the relation

$$H^2 = \frac{8\pi G}{3}\rho. \tag{1.15}$$

It is important to notice that Friedmann equations lead us to the continuity equation, via deriving Eq. (1.6) and then replacing Eq. (1.7), which gives us the evolution of energy density in an expanding universe, given by

$$\dot{\rho} + 3H(\rho + p) = 0, \tag{1.16}$$

and we notice that considering the equation of state and Eq. (1.15), this is consistent with Eq. (1.5), which is related to the conservation of the stress-energy tensor.

1.3 Early Universe Thermodynamics

Before going on to discuss the early radiation-dominated epoch of the universe, it is useful to recall some basic thermodynamical concepts, such as the number density n, energy density ρ, and pressure p of a particle species, as functions of the phase space distribution function $f(\vec{p})$:

$$n = \frac{g}{(2\pi)^3}\int f(\vec{p})d^3p, \tag{1.17}$$

$$\rho = \frac{g}{(2\pi)^3}\int E(\vec{p})f(\vec{p})d^3p, \tag{1.18}$$

$$p = \frac{g}{(2\pi)^3}\int \frac{|\vec{p}|^2}{3E}f(\vec{p})d^3p, \tag{1.19}$$

where we consider a weakly-interacting gas of particles with g internal degrees of freedom and $E^2 = |\vec{p}|^2 + m^2$. For a species in kinetic equilibrium, the phase distribution f is given by the well-known Fermi-Dirac or Bose-Einstein distributions:

$$f(\vec{p}) = \left[\exp\{((E-\mu)/T)\} \pm 1\right]^{-1}, \tag{1.20}$$

where μ is the chemical potential of the species, and here the plus and minus signs correspond to the Fermi-Dirac and Bose-Einstein species, respectively.

We see that in the relativistic limit ($T \gg m$) that the energy density satisfies $\rho \propto T^4$ then we can express the energy density and pressure of all species in equilibrium in terms of the photon temperature T as

$$\rho_R = T^4 \sum_{i=allspecies} \left(\frac{T_i}{T}\right)^4 \frac{g_i}{2\pi^2} \int_{x_i}^{\infty} \frac{(u^2 - x_i^2)^{1/2} u^2 du}{\exp\{(u - y_i)\} \pm 1}, \tag{1.21}$$

$$p_R = T^4 \sum_{i=allspecies} \left(\frac{T_i}{T}\right)^4 \frac{g_i}{6\pi^2} \int_{x_i}^{\infty} \frac{(u^2 - x_i^2)^{3/2} du}{\exp\{(u - y_i)\} \pm 1}. \tag{1.22}$$

where $x_i \equiv m_i/T, y_i \equiv \mu_i/T$, and T_i correspond to the species temperature, which could be different than that of the photons.

Since the energy density and pressure of a non-relativistic species are exponentially smaller than that of a relativistic species, it is very convenient and a good approximation to include only the relativistic species in Eqs. (1.21) and (1.22), in which case we obtain:

$$\rho_R = \frac{\pi^2}{30} g_* T^4, \tag{1.23}$$

$$p_R = \rho_R/3 = \frac{\pi^2}{90} g_* T^4, \tag{1.24}$$

where g_* counts the total number of effectively massless degrees of freedom. Its explicit expression is given by

$$g_* = \sum_{i=bosons} g_i \left(\frac{T_i}{T}\right)^4 + \frac{7}{8} \sum_{i=fermions} g_i \left(\frac{T_i}{T}\right)^4. \tag{1.25}$$

We see then that g_* is a function of T. For instance, for $T \ll MeV$, the only relativistic species are the 3 neutrino species and the photon so we have $g_* = 3.36$, where we have considered that the neutrino temperature is different from that of the photons. For $T \gtrsim 300GeV$, all the species in the standard model should have been relativistic and we obtain $g_* = 106.75$. We can see the dependence of $g_*(T)$ upon T in Fig. (1.2).

Another important concept to study in the history of the universe is entropy. Looking at the early stages, it is possible to consider that the reaction rates of particles in the thermal bath were much greater than the expansion rate H, and local thermal equilibrium should have been maintained, in this case, the entropy per comoving volume element should have remained constant, i.e.,

$$d(sR^3) = 0. \tag{1.26}$$

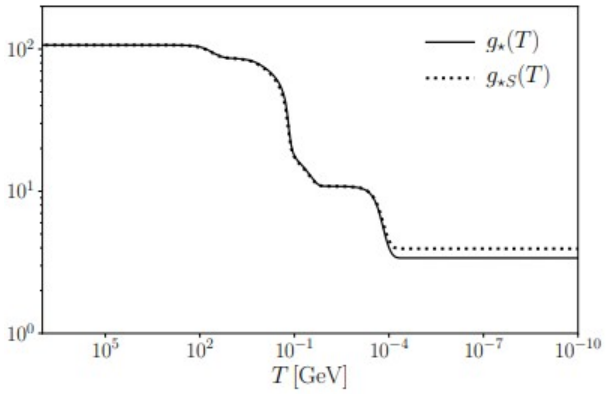

Figure 1.2: The evolution of $g_*(T)$ as a function of the temperature in the Standard Model [10].

Let us consider the second law of thermodynamics as well as the equilibrium expressions for the pressure and energy density, then we obtain the relation

$$dS = \frac{1}{T} d[(\rho + p)V] - \frac{V}{T} dp, \tag{1.27}$$

this allows us to relate the energy density and pressure:

$$dp = \frac{\rho + p}{T} dT, \tag{1.28}$$

replacing this expression in Eq. (1.27) we obtain that the entropy per comoving volume is given by $S = R^3(\rho + p)/T$, and using the energy conservation $d[(\rho + p)V] = V dp$, we obtain

$$d\left[\frac{(\rho + p)V}{T}\right] = 0 \tag{1.29}$$

which, defining the entropy density s as

$$s \equiv \frac{S}{V} = \frac{\rho + p}{T}, \tag{1.30}$$

proves Eq. (1.26).

We see now that since the entropy density is dominated by the contribution of relativistic particles, we could make the approximation

$$s = \frac{2\pi^2}{45} g_{*S} T^3, \tag{1.31}$$

where

$$g_{*S} = \sum_{i=bosons} g_i \left(\frac{T_i}{T}\right)^3 + \frac{7}{8} \sum_{i=fermions} g_i \left(\frac{T_i}{T}\right)^3. \tag{1.32}$$

Now, using Eq.(1.26) we can express the evolution of the temperature of the universe, in the form

$$\frac{ds}{dt} + 3Hs = 0. \tag{1.33}$$

which, written in terms of the scale factor R instead of time yields

$$\frac{dT}{dR} = -\left(1 + \frac{T}{3g_{*S}}\frac{dg_{*s}}{dT}\right)^{-1}\frac{T}{R}. \tag{1.34}$$

Finally, we can express Eq.(1.15) in terms of the temperature if we consider a universe dominated by radiation, Eq. (1.23), as

$$H(T) = \sqrt{\frac{\pi^2 g_*(T)}{30}\frac{T^4}{3M_P^2}} \tag{1.35}$$

where M_P is Planck's mass given by $M_P^2 = 1/8\pi G$. We can see from the conservation of entropy (Eq. (1.26)), that Eq. (1.31) allows us to relate the scale factor with the temperature at two different points, in relation to their entropy.

1.4 Big-Bang Nucleosynthesis

Primordial nucleosynthesis or Big-Bang nucleosynthesis (BBN) is one of the strongest supports to ΛCDM, in fact, is both the earliest and most stringent test of the theory, and an important probe of cosmology and particle physics. Today, the agreement between theory and observation indicates that the standard cosmology is a valid description of the Universe at least back to times as early as 10^2 s after the Big-Bang with temperatures as high as 10 MeV, where the Universe was dominated by radiation. It gives us numerous constraints on particle physics and cosmology, e.g., the abundance of light elements such as ^{4}He, D, ^{3}He in accordance with measures around 1% of precision. These predictions show great consistency with the observational data for ^{4}He and ^{7}Li, two isotopes whose abundance is barely affected by chemical and stellar evolution [11]. Furthermore, these isotopes determine the value of the baryon-to-photon ratio η to be of order 10^{-10} which also coincides with the data [12]. This matching between the data and the predictions, among other constraints [1], reveals that the universe had to be radiation dominated at BBN, although BBN is the cornerstone of the cosmological model, prior to this epoch stretches a period of cosmic history that is not completely constrained by observations. In the next chapters, we will look at this point and the theories that allow us to study physics beyond SM.

Chapter 2

Dark Matter Candidates

As we have mentioned before, the DM problem is one of the most important questions yet to be solved in modern physics. In this chapter, we will briefly discuss some of the most successful and promising DM candidates, in relation to their consistency with the conditions required to be considered as DM, their predictions with respect to the data obtained until today, and the mechanisms from which they are created in the early universe.

A few decades ago, it seemed reasonable to consider that DM might consist of substellar objects or stellar remnants, stars that simply were too faint to have yet been discovered. These candidates were named massive compact halo objects or MACHOs. But a combination of theory and observations have ruled them out to be able to solve de DM problem since, at best, they could be responsible for a small fraction of the DM in de Milky Way [13].

This allows us if we suppose the DM to be a particle, to consider that it must be nonbaryonic, and must have a good fit with the data associated with the CMB and BBN epoch. One of the most popular candidates is the weakly interacting massive particles (WIMPs). They arise naturally in various theories beyond SM, e.g., the neutralino in the minimal supersymmetric standard model [14], the Kaluza-Klein particle in models of universal extra dimensions [15] and the lightest particle in Little Higgs models [16]. It is important to stress that none of these models was proposed to solve de DM problem, the candidates come for free.

An important feature of WIMPs is that their mass range goes from 1 to 10^5 GeV [17]. The most outstanding observation is that the thermal production of WIMPs leads to the correct relic DM abundance (Eq. (1.14)) after their freeze-out from the thermal plasma, (if we assume they have weak-force interactions with the SM) which is usually referred to as the "WIMP miracle", moreover, the result is almost independent of the WIMP's mass and serves to motivate the interest in WIMP DM further.

Another promising candidate comes from considering an extra U(1) symmetry kinetically mixed with the electromagnetic U(1) of the SM. This corresponds to an extra photon-like particle, the so-called Hidden Photon (HP). The name comes from the idea that the interaction between these new particles and those of the SM is extremely weak, and their effects would simply be too feeble to have been observed yet, referred to belong to a so-called hidden sector. This candidate has been studied in various systems [18, 19, 20] and we will focus on a possible model where it constitutes the DM.

And last, but considered to be one of the most famous DM candidates, we have the Axion, or Axion-like Particles (ALPs). The first, initially proposed as a solution to the Strong-CP problem of Quantum Chromodynamics [21, 22]. The Axion is a (pseudo) Nambu-Goldstone boson that arises as a consequence

of the Peccei-Quinn mechanism.

The study of ALPs provides us with a better understanding of the production mechanisms and bounds related to their couplings and masses.

2.1 Production Mechanisms

Here we will do a brief review of some light DM production mechanisms, which gives us a different approach related to the relic abundance and the characteristic of the produced particles. First, we can consider thermal production. In [23] they studied the rate for thermal production of axions via the scattering of quarks and gluons and it is shown that the axion population can still be relativistic today. The production of thermal axions can be described by the Boltzmann equation and the interaction rate of all processes involving axions. It is found that the relic abundance depends on the thermal history of the universe, in the standard freeze-out scenario [24] and the production of thermal axions is too small and too hot to explain the DM in the typical scenario for the decay constant $F_a \simeq 10^{9-12}$ GeV [25].

There are also various studies related to DM production due to the decay of topological defects, formed after a phase transition during the early universe [26, 27, 28]. For some scenarios, DM from topological defects can account for the whole DM relic density, although those predictions are still under dispute [29, 30].

For the study related to this thesis, we are particularly interested in non-thermal production mechanisms due to the nature of the DM candidates. We will focus on bosonic candidates, who are susceptible to Bose-Enhancement effects [31, 32]. Since the DM candidate is required to be stable, i.e., having an average lifetime of at least the age of the universe (10^{17} s), the spontaneous decay rate can be used to set a restriction between their defining parameters, the mass and the coupling constant to other fields. This means that if we consider a DM candidate, which has a very low mass and a coupling that allows it to be sufficiently long-lived, we may require it to have enormous amounts of it to be able to deplete the DM energy density. One important feature of non-thermal production is that it could generate particles that are non-relativistic at the present time.

In the next section, we are going to present some very important features of the misalignment mechanism and how it allows us to consider a field that oscillates on time and has a very well-defined frequency. It is used in models related to axions and ALPs.

2.1.1 Misalignment Mechanism

Considering a simple Lagrangian density for a scalar field a, given by

$$\mathcal{L} = \frac{1}{2}\partial_\mu a \partial^\mu a - \frac{1}{2} m_a^2 a^2, \tag{2.1}$$

using the FRW metric we obtain the EoM to be

$$\ddot{a} + 3H\dot{a} + m_a^2 a - \frac{\nabla^2}{R^2} a = 0. \tag{2.2}$$

Here we can interpret that the field evolves with an oscillatory behavior with the presence of a damping term, which in certain regimes can give us an overdamped solution. We can now expand the field[1] $a(x)$ in its momentum modes

[1] In the following and for the sake of clarity we will refer to this field as axion, even though our only assumption has been is a scalar field, of a light mass.

$$a(x) = \int d^3k e^{ik\cdot x} a_k, \tag{2.3}$$

which gives us from Eq.(2.2)

$$\ddot{a}_k + 3H\dot{a}_k + \left(m_a^2 + \frac{k^2}{R^2}\right) a_k = 0. \tag{2.4}$$

Here it is important to consider two cases related to the momentum. For the modes outside the horizon, i.e., $k/R < H$, if we consider the regime where $m_a \ll H$, the EoM gives

$$\ddot{a}_k + 3H\dot{a}_k = 0, \tag{2.5}$$

and its solution is given by $a_k(t) = \alpha_1 + \alpha_2 t^{-1/2}$, which indicates that the dominant solution is a constant value and the modes of low momentum are considered to be frozen.

Then considering the momentum modes inside the horizon ($k/R > H$) the general solution for the EoM is given by

$$a_k = \frac{C}{R(t)} \cos\left(\int^t dt' \frac{k}{R(t')}\right). \tag{2.6}$$

We see here that since we are considering the regime for relativistic axions ($H, k/R \gg m_a$), the energy density satisfies $\rho_a \propto \dot{a_k}^2 \propto R^{-4}$, this indicates us that these correspond to relativistic modes, where axions dilute as radiation. Therefore, the above modes will just dilute with the expansion of the universe. The first modes, very close to the zero mode, froze outside the horizon, and keep their energy intact. These modes are the ones that can seed the dark matter particles.

We know that as the universe expands, H decreases so the frozen modes, i.e., the modes outside the horizon, eventually can enter the horizon, this happens approximately at $H \sim m_a$. In this case, we solve the EoM using a WKB approximation. Let us consider

$$a(t) = A(t)e^{i\phi(t)}, \tag{2.7}$$

which gives us from the EoM the equations for the Real and Imaginary parts to be

$$\frac{\ddot{A}}{A} - \dot{\phi}^2 + 3H\frac{\dot{A}}{A} + m_a^2 = 0, \tag{2.8}$$

$$\dot{A} + \left(\frac{\ddot{\phi}}{2\dot{\phi}} + \frac{3}{2}H\right) A = 0. \tag{2.9}$$

With WKB we consider the solution to have an amplitude that varies slowly in time, i.e., $(\frac{\ddot{A}}{A}, H\frac{\dot{A}}{A}) \ll \dot{\phi}$ so we can neglect the A derivative terms in Eq. (2.8) to obtain

$$\phi(t) = m_a t + C_1. \tag{2.10}$$

Replacing in Eq. (2.9) we obtain

$$A = \frac{C}{\sqrt{R^3 m_a}}, \tag{2.11}$$

so, finally, the solution for the field is given by

$$a(t) = \frac{C}{\sqrt{R^3 m_a}} \cos m_a t, \tag{2.12}$$

which as we expected, consists on an oscillatory field with a frequency equal to the mass of the field. If we take a look at the energy density of the axion field we see that considering $\rho_a \simeq \frac{1}{2} m_a^2 \langle a \rangle^2$ we obtain that $\rho_a \propto R^{-3}$ which is the same behavior as ordinary matter. Furthermore, if the universe evolves adiabatically, we obtained that since $R \propto T^{-1}$, we can relate the energy density with the temperature like $\rho_a \propto T^3$.

This mechanism also can give us the solution for the QCD axion, which has a temperature-dependent mass. The general solution is given by

$$a_{QCD}(t) = a_0 \sqrt{\frac{m_a(T_{osc}) R_{osc}^3}{m_a(T) R^3(T)}} \cos\left(\int dt' m_a(t') \right). \tag{2.13}$$

where T_{osc} is the temperature which satisfies $3H(T_{osc}) = m_a(T_{osc})$ which corresponds to the point where the field starts to oscillate, and $R_{osc} = R(T_{osc})$. The energy density is given by

$$\rho_a = \frac{1}{2} m_a^2 \langle a \rangle^2 \longrightarrow \rho_{a,0}(T_0) = \frac{1}{2} a_0^2 m_a(T_0) m_a(T_{osc}) \left(\frac{R_{osc}}{R_0} \right)^3. \tag{2.14}$$

Here we can use the expression for the entropy $S = sR^3$ which considering Eq. (1.31) gives us

$$S = \frac{2\pi g_{*S}(T)}{45} T^3 R^3. \tag{2.15}$$

We can now rearrange Eq. (2.14) to include the conservation of entropy given by

$$s_0 R_0^3 = s_{osc} R_{osc}^3 \rightarrow \left(\frac{R_{osc}}{R_0} \right)^3 = \frac{s(T_0)}{s(T_{osc})} = \frac{g_{*S}(T_0)}{g_{*S}(T_{osc})} \left(\frac{T_0}{T_{osc}} \right)^3. \tag{2.16}$$

Replacing the above relation in Eq. (2.14), and using Eq. (1.35) in the relation $3H(T_{osc}) = m_a(T_{osc})$ to express T_{osc}, we obtain, if we consider a constant mass for simplicity

$$\rho_a(T_0) = 0.13 \times 10^{-13} \text{ eV}^4 \left(\frac{a_0}{10^{11} \text{GeV}} \right)^2 \sqrt{\frac{m_a}{1\text{eV}}} \mathcal{F}(T_{osc}), \tag{2.17}$$

where $\mathcal{F}(T_{osc}) = (g_*(T_{osc})/3.36)^{3/4} (3.91/g_{*S}(T_{osc}) \sim 1$ [33]. This study allows us to connect the field's energy density with the actual DM abundance given by $\Omega_{DM,0} = 0.26$. Since we require the field to start oscillating before the matter-radiation equality ($T_e \sim 1.3$ eV), the mass is required to satisfy $m_a > 3H(T_e) = 1.8 \times 10^{-27}$ eV, which sets a bound to the model to obtain a result consistent with the current data, given by

$$\rho_{a,0} < 3.2 \times 10^{-15} \text{ eV}^4 \frac{m_a}{1 \text{ eV}} \left(\frac{a_0}{\text{TeV}} \right)^2. \tag{2.18}$$

This gives us a bound for the mass of the field.

We can also look at a more general form for the DM energy density, since we know that $\rho_{dm} \propto R^{-3}$, we

can use the relation between R and T for each cosmological epoch to express the DM energy density as a function of temperature. This feature and the effects of considering a different cosmological history in this relation are presented in the next chapter. For the DM energy density, considering the axion to be responsible for all the DM energy density, using Eq. (2.12) we can express

$$\rho_a = \rho_{dm}(R) = \rho_{dm,0}\left(\frac{R_0}{R}\right)^3, \tag{2.19}$$

where the subindex 0 indicates the value at the present time. This allows us to relate the DM energy density with the temperature. As mentioned before, if we consider the universe to evolve adiabatically, Eq. (1.31) gives us

$$\rho_{dm}(T) = \rho_{dm,0}\frac{g_{*S}(T)}{g_{*S}(T_0)}\left(\frac{T}{T_0}\right)^3, \tag{2.20}$$

where the term $\frac{g_{*S}(T)}{g_{*S}(T_0)}$ accounts for the point where the DM is produced. If we consider g_{*S} to be constant we can simplify this relation to

$$\rho_{dm}(T) = \rho_{dm,0}\left(\frac{T}{T_0}\right)^3. \tag{2.21}$$

It is relevant to mention that, since we have considered just a simple scalar field, this mechanism is valid for any scalar field that acquires a mass, for example by an explicit symmetry breaking.

At last, going back to DM production, another important mechanism to mention corresponds to the production of vector bosonic DM candidates, in [34, 35] they study vector DM production due to quantum fluctuations during inflation as Cosmic Strings and claim that this mechanism can account for all the DM density in the universe for some parameter space, in the form of a coherent oscillating condensate.

In the next chapter, we are going to present the possibility of considering a non-standard cosmological (NSC) scenario, its fundamental concepts, and its effects on the DM abundance.

Chapter 3

Non-Standard Cosmology

As mentioned before, ΛCDM assumes that prior to BBN, the universe transitioned from the inflationary epoch to an era dominated by radiation. Despite the great achievements of ΛCDM, there is scant evidence that supports this statement. This motivates us to study the dynamical evolution of DM through a period of non-standard cosmological (NSC) expansion, prior to BBN. The fact that to this day, the primordial abundances of helium and deuterium are measured with a 1% precision, makes BBN a powerful barrier, where the universe must transition into a radiation-dominated period. Despite this, we have motives to consider physics beyond SM, such as the unknown nature of inflation, dark energy, neutrino masses, and the DM, moreover, as the observations have become more precise, there have appeared some interesting points of current interest such as the Hubble tension [36], the tension on the power spectrum of density perturbations σ_s [37], among others. Those unsolved problems challenge the theory and motivate us to look at other possibilities.

It is possible to consider the existence of one or more additional fields that eventually could have happened to dominate the expansion of the universe. Some well-studied cases are Early Matter Domination (EMD) [38, 39] and Kination, i.e., kinetic energy domination [40, 41]. In this thesis, we will consider the existence of a field that potentially dominates the energy density of the universe in various scenarios. It is important to summarize a few important parameters.

3.1 NSC parameters

We will call the extra field ϕ and its equation of state is given by

$$p_\phi = \omega_\phi \rho_\phi. \tag{3.1}$$

As we mentioned before, is important to match the theory with BBN, i.e., we require the field not to dominate the expansion of the universe after $T_{BBN} \sim 1\,\text{MeV} \sim T_{end}$, since ΛCDM indicates a radiation dominated universe up to that point. The Boltzmann equations that govern the energy density of the field and the SM entropy density s are [42]

$$\frac{d\rho_\phi}{dt} + 3(1+\omega_\phi)H\rho_\phi = -\Gamma_\phi \rho_\phi, \tag{3.2}$$

$$\frac{ds}{dt} + 3Hs = \frac{\Gamma_\phi}{T}\rho_\phi. \tag{3.3}$$

where ρ_ϕ is the energy density of the ϕ field, Γ_ϕ is the decay rate of the ϕ field and s is the SM entropy density.

It is also important to recall that the Hubble parameter is given by

$$H = \sqrt{\frac{\rho_\phi + \rho_R + \rho_a}{3M_P^2}}, \tag{3.4}$$

where ρ_ϕ, ρ_R and ρ_a are the energy densities of ϕ, radiation and the axion field, respectively. Here we can neglect the axion contribution since it is always subdominant. It is useful to identify the temperature T_{end} where the field ϕ no longer dominates the energy density, which is related to the decay rate of the field and a temperature $T_{eq} > T_{end}$ in which the energy density of radiation and the field ϕ are equal, i.e., the moment at which ϕ starts to dominate the energy density after a radiation dominated period. This feature gives us the relation between the energy density and the scale factor as

$$\rho_R(R) = \rho_{eq}\left(\frac{R_{eq}}{R}\right)^4, \quad \rho_\phi(R) = \rho_{eq}\left(\frac{R_{eq}}{R}\right)^\beta, \tag{3.5}$$

where $\beta \equiv 3(1+\omega_\phi)$ and $R_{eq} = R(T_{eq})$. We have 2 possible scenarios; the first one is for $\beta < 4$, where the field ϕ is required to mostly decay up until T_{end} and the second, where $\beta > 4$, which means that the field does not require to decay since it dilutes itself as the universe expands [43] and we can consider the universe to be ϕ-dominated up until T_{end}.

Now, to determine T_{end} we have, for $\beta > 4$, that $\rho_\phi(T_{end}) = \rho_R(T_{end})$, and for a decaying field, this temperature corresponds to the point at which the field has mostly decayed, i.e., $H(T_{end}) = \Gamma_\phi$. Using Eqs. (1.15) and (1.23) this leads us to

$$T_{end}^4 \equiv \frac{90}{\pi^2 g_*(T_{end})} M_P^2 \Gamma_\phi^2. \tag{3.6}$$

We need also to consider the point where the approximation $\Gamma_\phi \ll H(T)$ is no longer valid due to the ϕ decay, we define then R_c which is the point where the decay of the field has an important impact in the evolution of the temperature. This requires solving Eqs. (3.2) and (3.3) considering $H(T) \approx \sqrt{\frac{\rho_\phi}{3M_P^2}}$, which, following the results found in [10, 43], at first order in Γ_ϕ/H_{eq} gives us

$$\rho_\phi(R) \approx \rho_{eq}\left[\left(\frac{R_{eq}}{R}\right)^\beta - \frac{2}{\beta}\frac{\Gamma_\phi}{H_{eq}}\left(\frac{R_{eq}}{R}\right)^{\beta/2}\right], \tag{3.7}$$

$$\rho_R(R) \approx \rho_{eq}\left[\left(\frac{R_{eq}}{R}\right)^4 + \frac{2}{8-\beta}\frac{\Gamma_\phi}{H_{eq}}\left(\frac{R_{eq}}{R}\right)^{\beta/2}\right], \tag{3.8}$$

as mentioned before, around H_{eq} the first term on the RHS of Eqs. (3.7) and (3.8) are the dominant ones. Considering that at R_c both terms in the RHS of Eq. (3.8) should be of the same order we obtain the relation

$$R_c \simeq R_{eq}\left(\frac{(8-\beta)}{2}\left(\frac{T_{eq}}{T_{end}}\right)^2\right)^{\frac{2}{8-\beta}}. \tag{3.9}$$

Also looking at Eq. (3.7), since the decay of ϕ should stop by the point in which both terms on the RHS become comparable, we obtain

$$R_{end} \simeq R_{eq}\left(\frac{\beta}{2}\left(\frac{T_{eq}}{T_{end}}\right)^2\right)^{2/\beta}. \tag{3.10}$$

then, we find the temperature T_c to be of the form

$$T_c \simeq T_{eq}\left(\frac{2}{8-\beta}\left(\frac{T_{end}}{T_{eq}}\right)^2\right)^{\frac{2}{8-\beta}}. \tag{3.11}$$

Finally from this analysis, we can extract that deep during the ϕ domination, the relation between temperature and scale factor is

$$T(R) \simeq T_{eq}\left[\frac{2}{8-\beta}\left(\frac{T_{end}}{T_{eq}}\right)^2\right]^{\frac{1}{4}}\left(\frac{R_{eq}}{R}\right)^{\frac{\beta}{8}}. \tag{3.12}$$

3.2 NSC effects on the expansion of the universe

As mentioned in the previous section, for a decaying field we have four different periods to consider in NSC, which, relating the Hubble parameter with the temperature, Eq. (1.35), yields

$$H(T) \simeq \begin{cases} H_R(T) & \text{for } T_{eq} \ll T, \\ H_R(T_{eq})\left(\frac{T}{T_{eq}}\right)^{\frac{\beta}{2}} & \text{for } T_c \ll T \ll T_{eq}, \\ H_R(T_{end})\left(\frac{T}{T_{end}}\right)^4 & \text{for } T_{end} \ll T \ll T_c, \\ H_R(T) & \text{for } T \ll T_{end}. \end{cases} \tag{3.13}$$

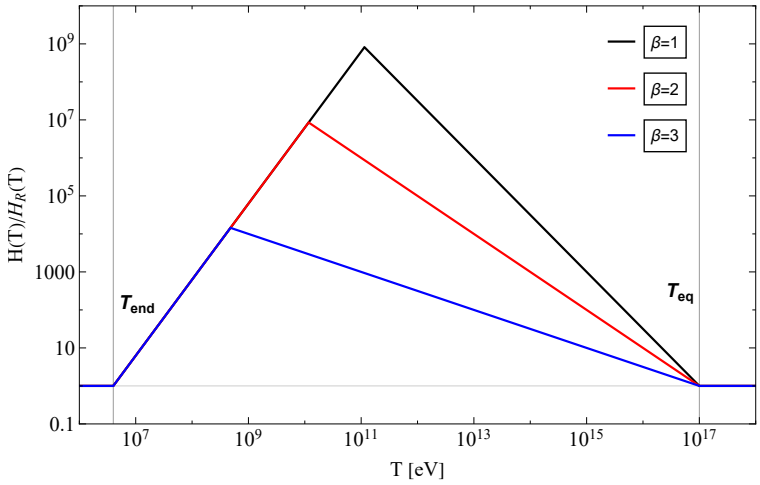

Figure 3.1: The evolution of the Hubble parameter normalized by the Radiation Hubble parameter (H_R) for different values of β, considering $T_{eq} = 10^8$ GeV and $T_{end} = 4$ MeV.

It is important to notice that since the temperature increases from left to right on the graphs, the cosmological history occurs from right to left since the temperature of the universe decreases in time. Also it es clear from Fig.(3.1) that fixing T_{eq} and T_{end} and varying β we also change T_c.

Whilst for a $\beta > 4$ we only have two important periods for NSC, and the relation between the Hubble parameter and the temperature is given by

$$H(T) \simeq \begin{cases} H_R(T_{end})\left(\frac{T}{T_{end}}\right)^{\frac{\beta}{2}} & \text{for } T_{end} \ll T, \\ H_R(T) & \text{for } T \ll T_{end}. \end{cases} \tag{3.14}$$

This indicates that the universe is ϕ-dominated before $T = T_{end}$, where starts the radiation-dominated period, this is shown in Fig. (3.2) for different values for β and $T_{end} = 4$MeV.

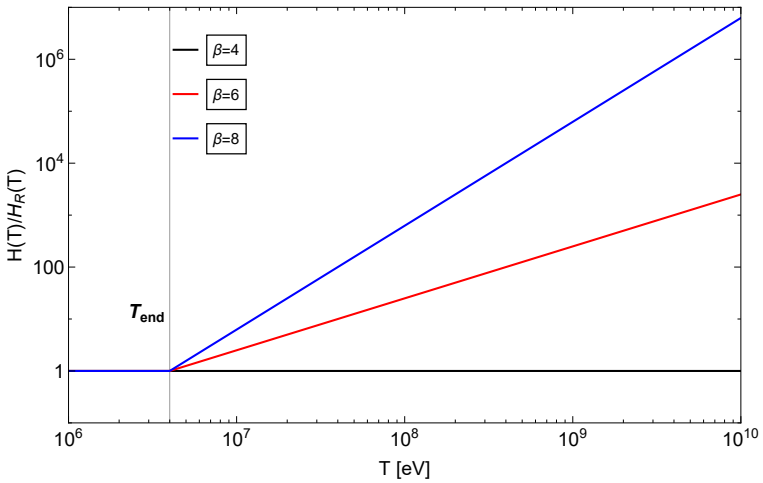

Figure 3.2: The evolution of the Hubble parameter normalized by the Radiation Hubble parameter (H_R) for different values of β, considering $T_{end} = 0.4$ GeV.

It is clear that for each value of β, we will obtain a different cosmological scenario. In the next chapter, we will analyze the effects of the variation of the expansion of the universe on the production of particles in systems affected by parametric resonance.

3.2.1 NSC effects on the DM energy density

The above relation between the scale factor and the temperature during the decay period (Eq. (3.12)) generates a different scheme for the DM energy density as a function of the temperature. We can understand it as follows, considering (2.19) and expressing explicitly the cosmological periods, we obtain

$$\rho_{dm}(R) = \rho_{dm,0}\left(\frac{R_0}{R}\right)^3 = \rho_{dm,0}\left(\frac{R_0}{R_d}\right)^3\left(\frac{R_d}{R_{end}}\right)^3\left(\frac{R_{end}}{R_c}\right)^3\left(\frac{R_c}{R}\right)^3, \tag{3.15}$$

where R_d corresponds to the scale factor at the time when the universe changes from radiation-dominated to matter-dominated, and we recall that R_{end} corresponds to the time where the ϕ field no longer dominates the energy density of the universe, and R_c corresponds to the time where starts the injection of entropy period. It is clear that for a SC regime, we have

$$\rho_{dm}(R) = \rho_{dm,0}\left(\frac{R_0}{R_d}\right)^3\left(\frac{R_d}{R}\right)^3. \tag{3.16}$$

Thus, if we evaluate the DM energy density in NSC at some moment prior to the start of the decay of the field, $R_p < R_c$, using Eq. (2.16) we get

$$\rho_{dm}(R_p) = \rho_{dm,0}\frac{g_{*S}(T_p)T_p^3}{g_{*S}(T_0)T_0^3}\frac{S_{\rm end}}{S_{\rm c}}. \tag{3.17}$$

where we have used $S_0 = S_{\rm d} = S_{\rm end}$ and $S_{\rm c} = S_p$. Therefore, the DM density evaluated at some moment before the decay of ϕ has a higher abundance than it would have in a standard, radiation-dominated expansion, due to the field's entropy injection into the thermal bath $S_{\rm end} > S_{\rm c}$, therefore, the DM energy density in NSC in the period prior to when ϕ have completely decayed is higher than the DM energy density in SC at the corresponding point. We see from Eq. (3.16) that in fact, that's the case since the

entropy S is conserved throughout all epochs, the extra term $S_{\rm end}/S_{\rm c}$ cancels out and we simply obtain Eq.(2.20).

It is important to mention that we are assuming that the DM density has been already set at this early moment described by R_p (and temperature T_p) and therefore is thermally and chemically decoupled from the primordial bath, thus does not share the entropy injection.

Another useful way to look at the DM density is as a function of the temperature, where we must include the injection of entropy period. This gives us for $\beta < 4$

$$\rho_{dm}(T) = \begin{cases} \rho_{dm,0}\left(\frac{T}{T_0}\right)^3 & \text{for } T \ll T_d, \\ \rho_{dm,d}\left(\frac{T}{T_d}\right)^3 & \text{for } T_d \ll T \ll T_{end}, \\ \rho_{dm,end}\left(\frac{T}{T_{end}}\right)^{24/\beta} & \text{for } T_{end} \ll T \ll T_c, \\ \rho_{dm,c}\left(\frac{T}{T_c}\right)^3 & \text{for } T_c \ll T \ll T_{eq}, \\ \rho_{dm,eq}\left(\frac{T}{T_{eq}}\right)^3 & \text{for } T_{eq} \ll T. \end{cases} \tag{3.18}$$

where $\rho_{dm,d} = \rho_{dm,0}\left(\frac{T_d}{T_0}\right)^3$, $\rho_{dm,end} = \rho_{dm,0}\left(\frac{T_{end}}{T_0}\right)^3$, $\rho_{dm,c} = \rho_{dm,0}\left(\frac{T_{end}}{T_0}\right)^3\left(\frac{T_c}{T_{end}}\right)^{24/\beta}$, and $\rho_{dm,eq} = \rho_{dm,0}\left(\frac{T_{eq}}{T_0}\right)^3\left(\frac{T_c}{T_{end}}\right)^{(24-3\beta)/\beta}$. We see the non-adiabatic period has a different behavior since the relation $R \propto T^{-1}$ is not satisfied. For NSC with $\beta > 4$, it is clear that, since there is no injection of entropy to the system, we simply have

$$\rho_{dm}(T) \propto T^3. \tag{3.19}$$

and this relation is satisfied at all cosmological times.

Summarizing, we are presented with two different scenarios. For $\beta > 4$ we have that the field ϕ simply dilutes itself as the universe expands and it dominates the energy density up until T_{end} where we return to ΛCDM. The other case occurs for $\beta < 4$ in which we have radiation domination up until T_{eq} where begins the ϕ-dominated period, at T_c begins the period of ϕ decaying and the entropy injection to the bath that ends up at T_{end}, which indicates that we go back to a radiation dominated universe and we connect with ΛCDM as well, these schemes are presented in Fig (3.1) and Fig. (3.2). In both cases, we see that the NSC period is completely defined by fixing three parameters, T_{end}, T_{eq}, and β.

Chapter 4

NSC effects on DM particle stability

In this section, we will look at the effects of considering a period of NSC before BBN in models where parametric resonance could have taken place during that non-standard expansion. We will first study a model where the DM particle is a hidden photon, coupled to an axion and a photon. Then, we will comment on a model with an ALP as the DM candidate, coupled with two HPs. A very important feature relies on the background field since in both cases we require its behavior to be that of an oscillatory field with a well-defined frequency, which is the case of the DM when produced via misalignment mechanism.

Parametric resonance is one of the crucial features present in the models studied, it presents itself as an effect produced by the interference of an external field, such as a background oscillatory field, which can allow a decay process. Parametric resonance has been widely studied in several models regarding axions (see [44, 45, 46, 47, 48]) and here we will look at some of the effects of considering a NSC history, related to the stability, particle production, and relic density of DM for different expansion rates of the early universe.

4.1 HP-DM coupled to axions and photons

Let us consider a Lagrangian invariant under the Z_2 symmetry and taking operators of at most mass dimension 5 given by

$$\mathcal{L} = -\frac{1}{4}F_{\mu\nu}F^{\mu\nu} - \frac{1}{4}F'_{\mu\nu}F'^{\mu\nu} + \frac{m'^2_\gamma}{2}A'_\mu A'^\mu + \frac{1}{2}\partial_\mu\phi\partial^\mu\phi - \frac{m^2_\phi}{2}\phi^2 + \frac{g_{\phi\gamma\gamma'}}{2}\phi F_{\mu\nu}F'^{\mu\nu}, \tag{4.1}$$

where ϕ is the ALP field, $g_{\phi\gamma\gamma'}$ is the HP-Axion-Photon coupling, F is the electromagnetic field strength of the SM, and F' is the corresponding one in the hidden sector. This model was studied in [20] to find the parameter space where the HP is found to be a viable DM candidate. Following this line of study, we will consider the HP field to constitute the DM, as a background field that decays into axions and photons.

One important feature of the model relies on the decay rate for the spontaneous decay process. If we consider the HP to be lighter than the axion ($m_{\gamma'} < m_\phi$), conservation of energy prevents the decay and the HP is considered stable. It is important to us when the HP can decay ($m_{\gamma'} > m_\phi$), but we require the HP to be stable, i.e., its average lifetime must be at least as large as the age of the universe. For this

model, it is given by

$$\tau = \frac{96\pi}{g^2_{\phi\gamma\gamma'} m^3_{\gamma'}} \left(1 - \frac{m^2_\phi}{m^2_{\gamma'}}\right)^{-3} \approx 2 \times 10^{17}\ \text{s} \left(\frac{g_{\phi\gamma\gamma'}}{10^{-6}\ \text{GeV}^{-1}}\right)^{-2} \left(\frac{m_{\gamma'}}{1\ \text{eV}}\right)^{-3}. \tag{4.2}$$

where in the last step, we have assumed $m_\phi \ll m_{\gamma'}$. Then considering the age of the universe, this gives us

$$\frac{g_{\phi\gamma\gamma'}}{1\ \text{eV}^{-1}} < 10^{15} \left(\frac{m_{\gamma'}}{1\ \text{eV}}\right)^{-3/2}. \tag{4.3}$$

This will constitute one of the bounds of the system in later analysis.

The Lagrangian in Eq. (4.1) gives us the EoM, using Lorenz gauge and considering terms such as $\propto \phi\vec{A}', \phi\vec{A}$ to be small, for the photon and the ALP field

$$(\partial_t^2 - \nabla^2)\vec{A} = -g_{\phi\gamma\gamma'} \nabla\phi \times \vec{E}'_{dm}, \tag{4.4}$$

$$(\partial_t^2 - \nabla^2 + m_\phi^2)\phi = -g_{\phi\gamma\gamma'} \vec{E}'_{dm} \cdot \vec{B}, \tag{4.5}$$

where considering that the hidden DM electric field can be written as $\vec{E}'_{dm} = E'_0 \cos m_{\gamma'} t \hat{\varepsilon}_{dm}$ and using the rotating wave approximation (see Appendix A.1 for more details), focusing on the process $\gamma' \to \gamma + \phi$ we obtain the equations for the photon and the axion to be

$$\partial_t a_k = \Omega_k \phi^\dagger_{-k} e^{-i\kappa t}, \tag{4.6}$$

$$\partial_t \phi^\dagger_{-k} = \Omega_k a_k e^{i\kappa t}, \tag{4.7}$$

where $\Omega_k = \eta \sin\theta \sqrt{\frac{k}{\omega_\phi}}$, $\eta = \frac{g_{\phi\gamma\gamma'} E'_0}{4}$, $\kappa = m_{\gamma'} - \omega - \omega_\phi$ and the frequencies are given by $\omega = k$, $\omega_\phi = \sqrt{k_\phi^2 + m_\phi^2}$. θ corresponds to the angle between the background HP polarization and the photon propagation. Here, since we focus on the decay process $\gamma' \to \gamma + \phi$ in the HP rest reference frame and considering a massless axion we obtain $k \approx m_{\gamma'}/2$.

We find the solutions for Eqs. (4.6) and (4.7) to be given by

$$a_k(t) = e^{\frac{-i\kappa t}{2}} \left[a_k(0) \left(\cos st + \frac{i\kappa}{2s} \sinh st\right) + \phi^\dagger_{-k}(0) \frac{\Omega_k}{s} \sinh st\right], \tag{4.8}$$

$$\phi^\dagger_{-k}(t) = e^{\frac{i\kappa t}{2}} \left[\phi^\dagger_{-k}(0) \left(\cos st + \frac{i\kappa}{2s} \sinh st\right) + a_k(0) \frac{\Omega_k}{s} \sinh st\right]. \tag{4.9}$$

where we have defined $s = \frac{1}{2}\sqrt{4\Omega_k^2 - \kappa^2}$. Since the process we are interested in is the decay of one HP into an axion and a photon, it is useful for us to look at the photon number density produced through the decay. First, we must look at the occupation number of photons given by

$$f_{\gamma,k}(t) = \frac{1}{V} \langle i|\, a_k^\dagger(t) a_k(t)\, |i\rangle\,. \tag{4.10}$$

Integrating over phase space we obtain the photon number density

$$n_\gamma(t) = \int \frac{d^3k}{(2\pi)^3} \left[f_{\gamma,k}(0) \left(\cosh^2(st) + \frac{\kappa^2}{4s^2} \sinh^2(st)\right) + f_{\phi,-k}(0) \frac{\Omega_k^2}{s^2} \sinh^2(st) + \frac{\Omega_k^2}{s^2} \sinh^2(st)\right]. \tag{4.11}$$

where $f_{\gamma,k}(0)$ and $f_{\phi,-k}$ are the initial number of photons and axions respectively. Here it is crucial to note that as long as s remains a positive real number, the number of photons produced due to the decay of the DM particle is parametrically amplified. This condition is translated as $-2\Omega_k < \kappa < 2\Omega_k$.

We can identify the first and second term of Eq.(4.11) as photon production due to stimulated HP decay triggered by an initial number of photons and axions respectively, while the third term corresponds to photon production due to spontaneous Bose-enhancement decay.

We assume the process happens such that there are no initial axions in the medium. On the other hand, we will see that this process is most important in the early universe, where the universe is filled with a thermal bath of photons, therefore, we will assume the photons are described by a thermal distribution given by

$$f_{\gamma,k}(0) = \frac{1}{e^{k/T} - 1}. \tag{4.12}$$

In this framework, we can integrate Eq. (4.11) for the number density of photons produced by the decay process, using a saddle point approximation (see Eq. (A.12) and that appendix for details) we find

$$n_\gamma(t) = \frac{m_{\gamma'}^2 \eta}{16\pi} \frac{e^{2\eta t}}{2\eta t} \left(f_{m_{\gamma'}/2} + \frac{1}{2} \right), \tag{4.13}$$

Here, $f_{m_{\gamma'}/2}$ is the initial occupation number of photons at energy $k \simeq m_{\gamma'}/2$. It is important to mention that, since we are considering $m_\phi = 0$, we can simplify the parameters $\Omega_k \simeq \eta \sin\theta$ and $\kappa = m_{\gamma'} - 2k$.

As mentioned before, since we are particularly interested in the resonant process, here it is crucial to look at the resonance window and its relation with the expansion of the universe (for a more detailed review on parametric resonance see Appendix B). A photon of frequency ω, which satisfies the resonance condition, is affected by the expansion of the universe and will have its wavenumber red-shifted, moving out the resonance window. The resonant decay of DM into axions and photons will happen if the DM condensate is excited by photons within a range δk, around the central value given by $k \simeq m_{\gamma'}/2$. We found in Appendix B that the size of the resonance window is $\delta k = 2\eta = 2\Omega_k$. Now we can relate the resonance window for the momentum with the Hubble parameter through

$$\delta k = \frac{m_{\gamma'} H \delta t}{2}, \tag{4.14}$$

which considering the resonance window gives us $\delta t = 4\Omega_k/(m_{\gamma'}H)$ and since we are interested in solutions exponentially increasing in time, we focus on the regime where the exponent $2\eta\delta t = g_{\phi\gamma\gamma'}^2 \rho_{dm}/(m_{\gamma'}H)$ increases in time. Furthermore, using the approximation $f_{m_{\gamma'/2}} \simeq 2T/m_{\gamma'}$, relating the DM density to the background amplitude by $E_0' = \sqrt{2\rho_{dm}}$, and taking the stability condition between the photon energy density and the DM density, which indicates us that ρ_{dm} must be greater than $\rho_\gamma = n_\gamma m_{\gamma'}/2$ we are able to find the bound for the coupling parameter to be

$$g_{\phi\gamma\gamma'}^2 < \frac{m_{\gamma'} H}{\rho_{dm}} \ln\left(\frac{64\pi\rho_{dm}}{\sqrt{2H m_{\gamma'}^5 T}} \right). \tag{4.15}$$

So far, we have assumed that the decay happens into massless photons, which is not true in the case of an astrophysical environment, where the photon acquires an effective mass due to plasma effects. Since the condition of Eq. (4.15) must be fulfilled at every cosmological epoch, we shall only consider hidden photons with a mass higher than the photon's mass, $m_{\gamma'} \geq m_\gamma$. Thus, to obtain the limit we will set $m_{\gamma'} = m_\gamma$, considering the plasma mass data for the photons obtained in [49]. Evaluating the expression (4.15), we obtain Figs. (4.1) and (4.2), where the region above the curve corresponds to unstable DM, i.e., a rapidly decaying DM. We implemented NSC considering $T_{end} = 4$ MeV, $T_{eq} = 10^8$ GeV, and $\beta = 3$, i.e., an early matter-dominated universe for Fig. (4.1), and $\beta = 6$ for Fig. (4.2). We will detail an approximated scheme to interpret the space parameter for the model and compare the behavior of the bound for SC and NSC. We also included the stability bound given by Eq. (4.3) as an orange dashed

line in both cases.

Let us first analyze the bound results for SC. Considering Eq. (4.15) to be mainly governed by the factor $m_{\gamma'}H/\rho_{dm}$, using Eqs. (1.35) and (2.21) we obtain that for a radiation-dominated period

$$g^2_{\phi\gamma\gamma'} \simeq m_{\gamma'}T^{-1}, \tag{4.16}$$

which extends across all periods considered for NSC and will be present in every analysis for the next sections.

4.1.1 NSC effects in the bound

It is very straightforward to take into account the effects of NSC, since as we mentioned in the previous chapter, the presence of an additional field dominating the energy density of the universe affects the Hubble parameter and the DM energy density in the early stages, which are both present in the bound for the coupling.

Let us first analyze the case $\beta < 4$. Since Eq. (4.15) is mainly governed by the expression outside the logarithm, we can focus on these terms. For example in the sector $T_c < T < T_{eq}$, looking at the Hubble parameter, we obtain from Eq. (3.13) that $H(T) \propto T^{\beta/2}$ whilst the DM energy density, considering Eq. (3.18) we obtain $\rho_{dm}(T) \propto T^3$, ultimately, and using the expression found in [50] for the relation between the plasma mass with the temperature at early stages given by $m_{\gamma'} \propto T$, we obtain $g_{\phi\gamma\gamma'} \propto m_{\gamma'}^{(\beta-4)/4}$. This allows us to interpret the curve in Fig. (4.2) for the different periods of NSC. An approximated scheme that contains a non-adiabatic period is given by

$$g_{\phi\gamma\gamma'}(m_{\gamma'}) \propto \begin{cases} m_{\gamma'}^0 & \text{for } T_{eq} \ll T, \\ m_{\gamma'}^{(\beta-4)/4} & \text{for } T_c \ll T \ll T_{eq}, \\ m_{\gamma'}^{(3\beta-24)/2\beta} & \text{for } T_{end} \ll T \ll T_c, \\ m_{\gamma'}^0 & \text{for } T \ll T_{end}. \end{cases} \tag{4.17}$$

We can see then that, for example in early matter domination ($\beta = 3$), the curve for the bound is expected to restrict a wider space of parameters since the dependence on the HP mass drops from an exponent 0 in the radiation-dominated period to -1/4 in the non-adiabatic period of ϕ-dominated period, to then behave with exponent -5/2 up until the radiation-dominated epoch at the earlier time where it goes back to a constant behavior if we neglect the logarithm term in the bound. It is important to mention that since we are considering the plasma mass data displayed in [49], the results shown are restricted by the data range for the plasma mass.

Considering this analysis we can see for $\beta < 4$ (Fig. 4.2) that in fact, these effects translate as a greater bound for the coupling constant, i.e., it gives us a wider sector of prohibited values for $g_{\phi\gamma\gamma'}$ for greater plasma masses. This tells us that to consider a viable HP-DM with masses over 10^5 eV in NSC we will require a smaller coupling constant to avoid the unstable period of the system, although this mass value interferes with the spontaneous decay requirement to consider a stable and long-lived DM of at least the age of the universe which is a crucial requirement for the model. We will address this at the end of the section.

On the other hand, since the Hubble parameter and the DM energy density have different expressions in NSC with $\beta > 4$, we must do the corresponding analysis. Considering Eqs. (3.14), (3.19) and again

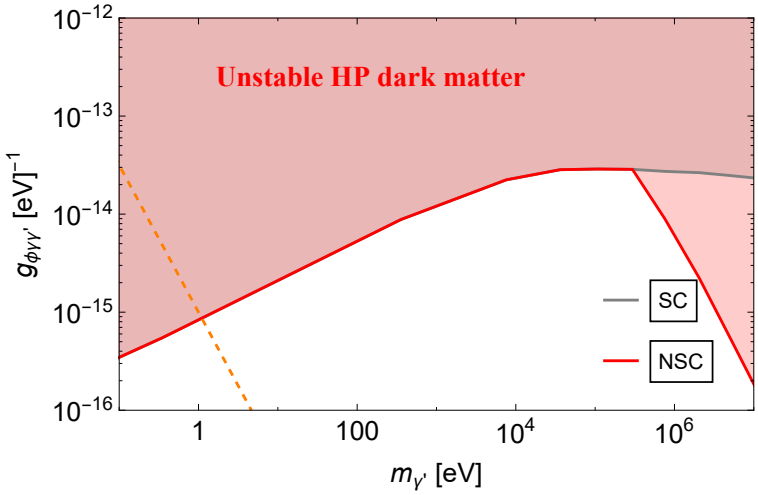

Figure 4.1: Exclusion plot for the coupling constant for NSC with $\beta = 3$. To the right of the orange dashed line, the model is excluded by the perturbative decay rate presented in Eq.(4.3).

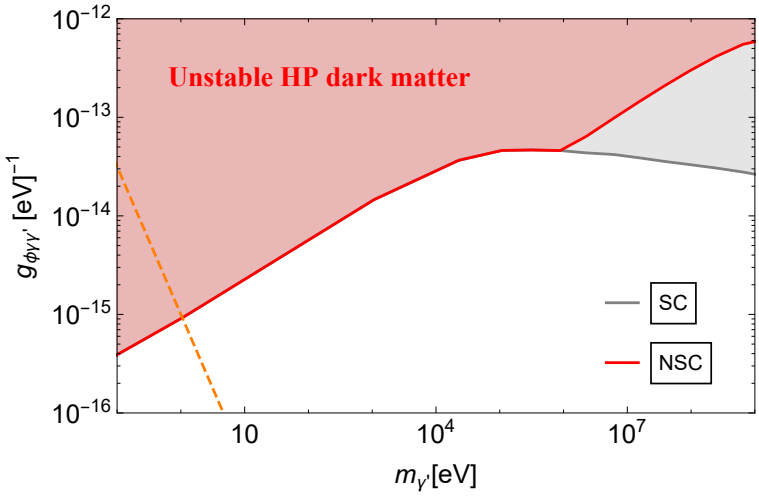

Figure 4.2: Exclusion plot for the coupling constant for NSC with $\beta = 6$. To the right of the orange dashed line, the model is excluded by the perturbative decay rate presented in Eq.(4.3).

the relation of the plasma mass with the temperature, we obtain

$$g_{\phi\gamma\gamma'}(m_{\gamma'}) \propto \begin{cases} m_{\gamma'}^{(\beta-4)/4} & \text{for } T_{end} \ll T, \\ m_{\gamma'}^{0} & \text{for } T \ll T_{end}. \end{cases} \tag{4.18}$$

This shows that for values of $\beta > 4$, the slope of the bound is positive in the NSC period, so it gives us a wider parameter space for stable HP-DM, which is the opposite of the result obtained for the previous analysis.

In consistency with this relation, we note that if we implement NSC with $\beta > 4$ (Fig. 4.2) we see that the bound is less restricted, allowing bigger values for the coupling constant for higher values of plasma mass, in correspondence with the scheme presented in Eq. (4.18) where we see for greater values of β, the prohibited parameter space gets smaller in the NSC period, although as mentioned before, bigger masses for the HP could make it susceptible to decay spontaneously, ruining its stability.

We must then consider the bound related to the spontaneous decay rate, which relates the coupling

constant and the DM particle mass to assure its stability. In Fig. 4.2 we see this bound in both scenarios for β as the orange dashed line. We see that the NSC period occurs in the sector that provides unstable particles, then, although the NSC effects are found and consistent with the analysis, they occur in a sector where the model isn't capable of solving the DM problem. We will then study where this restriction related to the plasma mass is not an issue to implement a NSC.

4.2 ALP decay to two hidden photons

As we have mentioned, there is a high motivation for the study of an ALP DM candidate coupled to two photons in a great variety of systems. Here we will consider a similar scenario. Axions and ALPs are one of the most popular DM candidates, which are very light and weakly coupled and they can in principle decay. However, if both their couplings and mass are small, they contribute to the decay rate being extremely small and thus may be of little concern. However, in general, we see that this set a bound between the mass and the coupling constant. We will see from our analysis that since the mass is an important parameter to express the bound that we must take into consideration this relation for the DM stability.

Let us now consider a system that has a coupling of an ALP to two massless HP, whose Lagrangian density is given by

$$\mathcal{L} = \frac{1}{2}(\partial_\mu \phi)^2 - \frac{1}{2}m_\phi^2 \phi^2 - \frac{1}{4} g_{\phi\gamma'\gamma'} \phi F'^{\mu\nu} \tilde{F}'_{\mu\nu}. \tag{4.19}$$

where $g_{\phi\gamma'\gamma'}$ is the coupling constant of the ALP to HPs, $F'^{\mu\nu}$ is the HP field strength and $\tilde{F}'_{\mu\nu}$ is its dual. The perturbative decay rate is given by

$$\Gamma_{pert} = \frac{g_{\phi\gamma'\gamma'}^2 m_\phi^3}{64\pi}. \tag{4.20}$$

Looking at its stability, we require that for ϕ to be stable that $\Gamma_{pert} < H_0$, where H_0 is the present-day Hubble parameter. This gives us the stability bound to be

$$\frac{g_{\phi\gamma'\gamma'}}{10^{16}\ \mathrm{eV}^{-1}} < 5 \times \left(\frac{m_\phi}{1\ \mathrm{eV}}\right)^{-3/2}. \tag{4.21}$$

The perturbative decay rate is in fact really tiny in a great range of masses, but we still need to pay attention to this decay process. The reason lies in the ALP DM production mechanism since as mentioned before, the particles produced by misalignment are highly coherent, they are produced in the same state and therefore their occupation number is enormous. This makes Bose enhancement effects plausible. Considering the spontaneous decay of the ALPs, it is possible for Bose enhancement decay to occur. Similar to the previous section, we will take into account the effect of the expansion of the universe on the modes of the particles produced via decay and then we will analyze the effects on NSC scenarios.

Considering Eq. (4.19), the EoM for the HP in a homogeneous axion background can be written as

$$(\partial_t^2 - \nabla^2)\vec{A}' = -g_{\phi\gamma'\gamma'} \partial_t \phi \vec{\nabla} \times \vec{A}', \tag{4.22}$$

$$(\partial_t^2 + m_\phi^2)\phi = g_{\phi\gamma'\gamma'} \partial_t \vec{A}' \cdot \vec{\nabla} \times \vec{A}'. \tag{4.23}$$

In this case, we consider the HP as a plane and linearly-polarized electromagnetic wave of frequency ω, and the background axion field is taken to have the form $\phi(t) = \phi_0 \cos m_\phi t$. We could also use the rotating wave approximation (see Appendix A.2 for more details) and focus on the relevant process of the system, which corresponds to the decay $\phi \to \gamma' + \gamma'$. We obtain the equations for the polarizations of the HPs to be

$$\partial_t A'_{k,\pm} = \pm \frac{1}{4} g_{\phi\gamma'\gamma'} m_\phi \phi_0 e^{i\kappa t} A'^{\dagger}_{-k,\pm}, \tag{4.24}$$

$$\partial_t A'^{\dagger}_{-k,\pm} = \pm \frac{1}{4} g_{\phi\gamma'\gamma'} m_\phi \phi_0 e^{-i\kappa t} A'^{\dagger}_{k,\pm}. \tag{4.25}$$

Here, for simplicity, we will focus on the "+" polarization (the following analysis is also valid for the "−"

polarization), and we see that it is possible to compare these differential equations to Eqs. (4.6) and (4.7), obtained in the previous section. We can identify $\Omega_k = \frac{1}{4} g_{\phi\gamma'\gamma'} m_\phi \phi_0$ and $\{a_k, \phi^\dagger_{-k}\} \to \{A'_{k,+}, A'^\dagger_{-k,+}\}$, moreover, the energy conservation relation gives us $\kappa = m_\phi - \omega_{\gamma'} - \omega_{\gamma'}$. Therefore, Eqs. (4.25) and (4.24) have the same form as the ones found in the previous model, and thus, their solution is formally the same, meaning

$$A'_{k,+}(t) = e^{\frac{i\kappa t}{2}} \left[A'_{k,+}(0) \left(\cosh st + \frac{i\kappa}{2s} \sinh st \right) + \frac{\Omega_k}{s} A'^\dagger_{-k,+}(0) \sinh st \right], \tag{4.26}$$

$$A'^\dagger_{-k,+}(t) = e^{\frac{-i\kappa t}{2}} \left[A'^\dagger_{-k,+}(0) \left(\cosh st - \frac{i\kappa}{2s} \sinh st \right) + \frac{\Omega_k}{s} A'_{k,+}(0) \sinh st \right], \tag{4.27}$$

where $s = \frac{1}{2}\sqrt{4\Omega_k - \kappa^2}$ and $A'_{k,+}(0), A'^\dagger_{-k,+}(0)$ are the initial conditions of the system. This solution allows us again to define the number density, this time for the " + "-polarized-HPs, using Eqs. (A.28) and (A.29). We want to consider the effect of parametric decay at every epoch, so we will make the reasonable assumption that there is no initial population of hidden photons to trigger the enhanced decay of the dark matter. Instead, we will be looking at the 'spontaneous process', even though, once it happens, HPs produced by the spontaneous decay will induce the stimulated decay due to the bosonic nature of the particles. This allows us to consider an initial state with no initial occupation number of axions or neither of the HP's polarization, which left us with a density number composed only for the Bose-enhancement term of the decay, which corresponds to

$$n_+ = \int \frac{d^3k}{(2\pi)^3} \frac{\Omega_k^2}{s^2} \sinh^2 st, \tag{4.28}$$

This gives us, considering the regime $st \gg 1$ and the saddle point approximation for the HP number density to be

$$n_+(t) = \frac{m_\phi^2}{128\pi} \sqrt{\frac{\Omega_k}{\pi t}} e^{2t\Omega_k}, \tag{4.29}$$

where we can recall $2\delta t \Omega_k = g^2_{\phi\gamma'\gamma'} \rho_{dm} / m\phi H$. Similar to the previous model, we can relate the resonance band for the system with the expansion of the universe using Eq. (4.14) to obtain the expression for the bound of the system to be

$$g^2_{\phi\gamma'\gamma'} < \frac{m_\phi H}{\rho_{dm}} \ln \left(\frac{128\pi\rho_{dm}}{\sqrt{H m_\phi^7 / \pi}} \right). \tag{4.30}$$

In the following, we will take into consideration one very important feature of the model. We will work under the assumption the ALP DM has been produced by the very well-known misalignment mechanism. Therefore, in order to evaluate the bound, similar to the analysis realized in the previous model, we will find an expression for the energy density as a function of the temperature.

4.2.1 NSC effects in the bound

Let us first focus on the term outside the logarithm in Eq. (4.30), with a constant value for the ALP mass and taking into consideration the dependence of the Hubble parameter and the DM energy density. We see that for NSC with $\beta < 4$

$$\frac{H(T)}{\rho_{dm}(T)} \propto \begin{cases} T^{-1} & \text{for } T_{eq} \ll T, \\ T^{(\beta-6)/2} & \text{for } T_c \ll T \ll T_{eq}, \\ T^{(4\beta-24)/\beta} & \text{for } T_{end} \ll T \ll T_c, \\ T^{-1} & \text{for } T \ll T_{end}. \end{cases} \tag{4.31}$$

We can see clearly that the function is strictly decreasing as the temperature increases, this allows us to simplify the analysis due to the fact that since we are looking at the biggest restriction for the coupling that satisfies Eq.(4.30), we have to consider the lowest possible value for H/ρ_{dm}. This means that for each mass, we must evaluate the bound in the highest value of temperature. Here we must include the features of the production mechanism. We considered the misalignment mechanism to be responsible for the background ALP field, then we need to look at the temperature at which the system starts to oscillate and the relation between the Hubble parameter and the mass field. From Sec. 2.1.1 we see that the system starts to oscillate at a temperature T_{osc} that satisfies

$$3H(T_{osc}) \simeq m_\phi. \tag{4.32}$$

then the highest possible value of T is given by T_{osc} and we can reparametrize the bound as a function solely of the ALP mass, using the relation between the DM energy density and the Hubble parameter. A general scheme for the coupling is given by

$$g_{\phi\gamma'\gamma'} \propto \begin{cases} m_\phi^{1/4} & \text{for } T_{eq} \ll T, \\ m_\phi^{(2\beta-6)/2\beta} & \text{for } T_c \ll T \ll T_{eq}, \\ m_\phi^{(2\beta-6)/2\beta} & \text{for } T_{end} \ll T \ll T_c, \\ m_\phi^{1/4} & \text{for } T \ll T_{end}. \end{cases} \tag{4.33}$$

Another important point to mention relies on the fact that we can interpret from the previous analysis that this process of resonant decay is more efficient at earlier times, then the NSC effect may be particularly relevant.

We can now interpret the results in relation to the parameter space. We see that in the radiation-dominated era, the bound is proportional to $m_\phi^{1/4}$, and in the ϕ-dominated period, its exponent drops depending on β, but it is clear that the result always prohibits a wider space of parameters. One important case to mention corresponds to early matter domination, where we see that the dominant term on the bound does not depend on the ALP mass and behaves as a constant value. Also, as we mentioned in the previous model, it is important to take into consideration the stability condition from the spontaneous decay process given by Eq. (4.21). This relation between the ALP mass and the coupling constant is illustrated in Figs. 4.3 and 4.4 as the orange dashed line.

Now looking at the cases with $\beta > 4$, we obtain the scheme to be

$$\frac{H(T)}{\rho_{dm}(T)} \propto \begin{cases} T^{(4\beta-24)/\beta} & \text{for } T_{end} \ll T, \\ T^{-1} & \text{for } T \ll T_{end}. \end{cases} \tag{4.34}$$

here we can notice that in the opposite of the previous case, for sufficiently large β the function H/ρ_{dm} can decrease as the temperature drops, but this sector is prohibited by the stability condition so we can still rely on the highest value of temperature to find the greater bound. Now we can implement the relation between the ALP mass and the Hubble parameter to express the coupling in terms of the ALP mass. For this model, it is given by

$$g_{\phi\gamma'\gamma'} \propto \begin{cases} m_\phi^{(2\beta-6)/2\beta} & \text{for } T_{end} \ll T, \\ m_\phi^{1/4} & \text{for } T \ll T_{end}. \end{cases} \tag{4.35}$$

where in this case we see that for $\beta > 4$ the exponent on the ϕ-dominated period is greater than $1/4$, we expect then that the bound of the model will present a wider area of permitted coupling values for

greater masses. Once again we must take into consideration the stability condition of the DM candidate due to spontaneous decay and intersect both restrictions to obtain the allowed parameter space for the model.

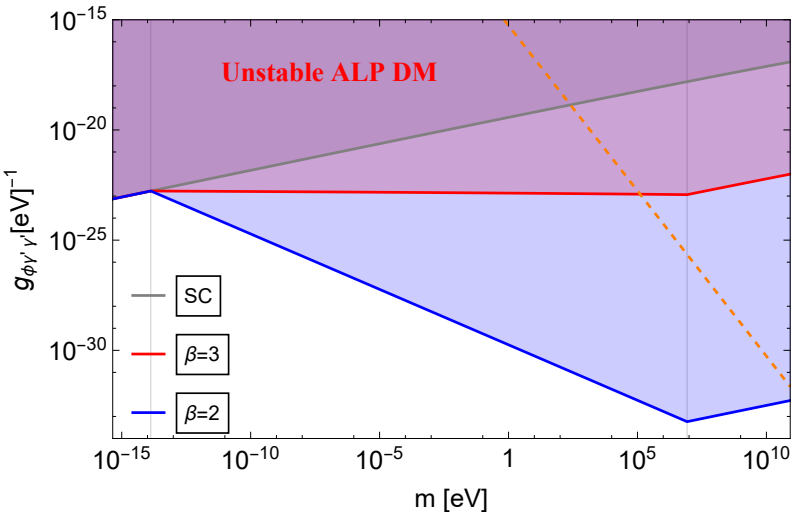

Figure 4.3: The parameter space for the coupling of an ALP to two HPs in SN and NSC for $\beta < 4$. To the right of the orange dashed line, the model is excluded by the perturbative decay rate presented in Eq.(4.21).

Let us now compare the result shown in Fig. 4.3 with the analysis previously mentioned. We see that in the period of NSC for $\beta < 4$ that the bound is stronger than the one obtained from SC, giving a wider sector for prohibited parameters, especially for smaller values of β, we see that the case of EMD, i.e., NSC with $\beta = 3$ shows a particular behavior since the bound does not depend on the mass of the ALP. In relation to the stability condition due to spontaneous decay, given by Eq. (4.21) and shown in Figs. 4.3 and 4.4 as the orange dashed line, we see that a certain area of NSC is ruled out, but we are still presented with a viable parameter space, where NSC effects present a different scenario.

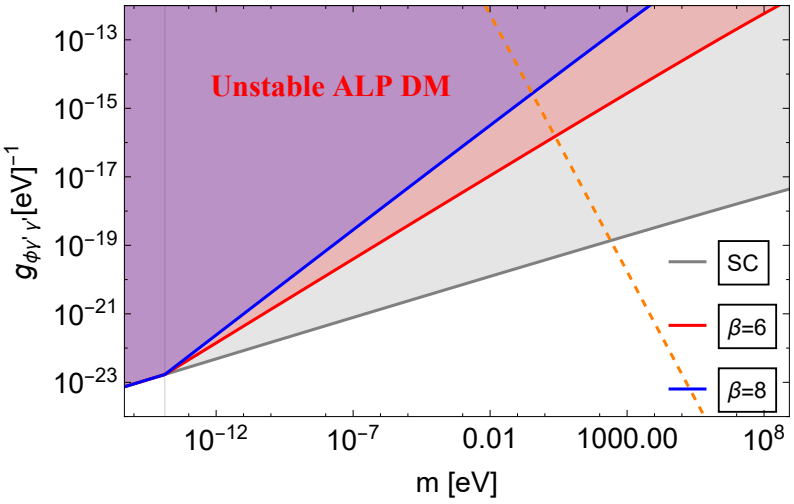

Figure 4.4: The parameter space for the coupling of an ALP to two HPs in SN and NSC for $\beta > 4$. To the right of the orange dashed line, the model is excluded by the perturbative decay rate presented in Eq.(4.21).

On the other hand, if we look at Fig. (4.4), NSC gives us a weaker restriction for the coupling constant

since the unstable sector is smaller for greater values of β, which is consistent with the previous analysis. Once again looking at the stability condition, we see that a certain area of NSC is ruled out but we are still presented with a wide parameter space viable for the model and we can consider higher masses to be stable in a wider range of the coupling constant if we consider NSC.

4.3 Further models

This type of analysis allows us to consider future applications to other systems studied in the literature. As we saw in both systems analyzed, we can take into consideration the particle production of systems with parametric resonance to relate the expansion of the universe with the resonance window. This is very useful since there are a great variety of physical systems that presents this feature and can show the effects of considering a NSC period. One model of particular interest corresponds to the model studied in [51] as a toy model with an interaction Lagrangian of the form

$$\mathcal{L}_I = g\phi\chi^2. \tag{4.36}$$

this is similar to the model of the ALP-2HPs but presents an alternative approach using Floquet theory to analyze the resonant decay of the ϕ background, instead of using the rotating wave approximation as we did.

There is also interest in the model in [52] where they look at the stability of millicharged light bosonic DM with a Lagrangian of the form

$$\mathcal{L} = -\frac{1}{4}F^2 + (D_\mu\phi)^\dagger D^\mu\phi - m^2\phi^\dagger\phi. \tag{4.37}$$

and its decay into photons.

There are also various models in (p)reheating related to inflation [53, 54, 55] or DM production [56], among others, which can be interesting objects of study.

Conclusions

In this thesis, we have studied the effects on the stability of DM candidates due to the implementation of a NSC period prior to BBN. This means that instead of a simple extrapolation of the radiation-dominated period that stipulates ΛCDM, we have considered a period in which the universe was dominated for a new field ϕ. This allowed us to study the effects that NSC produced on the expansion of the universe as well as the DM energy density and its relic value. We have shown the difference between different equations of state for the new field and we established the necessary parameters to describe the NSC period.

We have found two important regimes, first for $\beta < 4$ we have that the additional field must decay before BBN, thus the DM energy density must be higher in early times compared to SC to match the data at the present day due to the fact that an additional field dominating the universe would dilute the DM density. On the contrary, for $\beta > 4$ we have found that since the universe expands faster, the DM density must be smaller in NSC. Then we implemented NSC to two different DM models affected by parametric resonance. The first one consisted of a HP-DM coupled to an axion and a photon, we solved the equations of motion in the resonance frame and we relate the expansion of the universe with the resonance window of the system. Then we found the number density of photons produced by the HP decay and determine the stable parameter space, capable of accounting for the total DM density but the result showed that the NSC effects would occur for particles with masses that are prohibited by the stability condition due to spontaneous decay of the candidate.

Then we implemented NSC in a model of an ALP-DM coupled to two massless HPs and again solved the equations of motion for the resonant decay process to find the stability bound of the system taking into account the production mechanism to obtain an exclusion plot where we found that NSC for $\beta < 4$, we considered an early matter-dominated universe and obtained that this gives us a stronger bound for the coupling, prohibiting a wider sector of masses whilst NSC for $\beta > 4$ we obtained that the exclusion plot gives a smaller prohibited area of parameters, allowing a wider combination of coupling and ALP mass to be able to describe the DM energy density. For this model, the results were compatible with the stability condition due to spontaneous decay so we defined a viable space of parameters to consider this model as a DM candidate.

It is important to mention that the models studied have several other restrictions related to observations, astrophysical tests, and a wide variety of experiments, that were not mentioned in the discussion for the sake of clarity in the study. Nevertheless, in light of the obtained results in this thesis, it seems useful to consider the study of the parameter space of models with DM candidates under the supposition of a period of non-standard expansion prior to BBN in a complete setup. This investigation seems interesting as a future extension to this work.

Appendix A

Rotating Wave Approximation

A.1 HP to Axion-Photon system

Taking into account the Eqs. (4.4) and (4.5) and considering the axion field and the photon field given by

$$A(x,t) = \int \frac{d^3k}{(2\pi)^3}\frac{1}{\sqrt{2\omega}}\left[a_k(t)e^{i(\vec{k}\cdot\vec{x}-\omega t)} + a_k(t)^\dagger e^{-i(\vec{k}\cdot\vec{x}-\omega t)}\right], \tag{A.1}$$

$$\phi(x,t) = \int \frac{d^3k}{(2\pi)^3}\frac{1}{\sqrt{2\omega_\phi}}\left[\phi_k(t)e^{i(\vec{k}\cdot\vec{x}-\omega_\phi t)} + \phi_k(t)^\dagger e^{-i(\vec{k}\cdot\vec{x}-\omega_\phi t)}\right], \tag{A.2}$$

where $\omega_\phi = \sqrt{k^2+m_\phi^2}$, $\omega = k$. Moreover, we assume that the amplitudes $a_k(t)$ and $\phi_k(t)$ vary slowly in time so we can neglect the second derivative term in the EoM, and they satisfy the commutation relations given by $[\phi_k(t), \phi^\dagger_{k'}(t)] = [a_k(t), a^\dagger_{k'}(t)] = (2\pi)^3\delta^3(k-k')$. Using the rotation wave approximation we obtain the coupled system given by

$$\partial_t a_k = \eta sin\theta\sqrt{\frac{k}{\omega\phi}}\left(\phi_k e^{-i\Delta_1 t} + \phi_k e^{-i\Delta_2 t} + \phi^\dagger_{-k}e^{-i\kappa t}\right), \tag{A.3}$$

$$\partial_t \phi_k = -\eta sin\theta\sqrt{\frac{k}{\omega\phi}}\left(a_k e^{i\Delta_1 t} + a_k e^{i\Delta_2 t} - a^\dagger_{-k}e^{-i\kappa t}\right), \tag{A.4}$$

where we defined $\Delta_1 = m_{\gamma'} + \omega - \omega_\phi, \Delta_2 = m_{\gamma'} - \omega + \omega_\phi$ and $\kappa = m_\phi - \omega - \omega_\phi$. It is important to mention that θ corresponds to the angle between the photon propagation and that of the HP background polarization. This gives us, if we consider only the process $m_{\gamma'} \to \omega + \omega_\phi$, the following set of equations

$$\partial_t a_k = \Omega_k \phi^\dagger_{-k} e^{-i\kappa t}, \tag{A.5}$$

$$\partial_t \phi^\dagger_{-k} = \Omega_k a_k e^{i\kappa t}. \tag{A.6}$$

Here we have defined $\Omega_k = \eta \sin\theta\sqrt{\frac{k}{\omega_\phi}}$ and we can see that κ represent the energy conservation relation of the resonant process. The solutions for Eqs. (A.5) and (A.6) are given by

$$a_k(t) = e^{-i\kappa t/2}\left[a_k(0)\left(\cosh(st) + i\frac{\kappa}{2s}\sinh(st)\right) + \phi^\dagger_{-k}(0)\frac{\Omega_k}{s}\sinh(st)\right], \tag{A.7}$$

$$\phi^\dagger_{-k}(t) = e^{i\kappa t/2}\left[\phi^\dagger_{-k}(0)\left(\cosh(st) - i\frac{\kappa}{2s}\sinh(st)\right) + a_k(0)\frac{\Omega_k}{s}\sinh(st)\right]. \tag{A.8}$$

Here $s = \frac{1}{2}\sqrt{4\Omega_k^2 - \kappa^2}$. This solution allows us to define the occupation number for ϕ-particles and a-particles.

$$f_{\phi,k}(t) = \frac{1}{V}\langle i|\,\phi^\dagger_k(t)\phi_k(t)\,|i\rangle\,, \tag{A.9}$$

$$f_{\gamma,k}(t) = \frac{1}{V}\langle i|\,a^\dagger_k(t)a_k(t)\,|i\rangle\,. \tag{A.10}$$

which, after replacing Eq. (A.7) for the photon occupation number gives us

$$f_{\gamma,k}(t) = f_{\gamma,k}(0)\left(\cosh^2(st) + \frac{\kappa^2}{4s^2}\sinh^2(st)\right) + f_{\phi,-k}(0)\frac{\Omega_k^2}{s^2}\sinh^2(st) + \frac{\Omega_k^2}{s^2}\sinh^2(st). \tag{A.11}$$

where $f_{\gamma,k}(0)$ and $f_{\phi,-k}(0)$ are the initial occupation number of photons and axions respectively. Finally, we obtain the photon number density

$$n_\gamma(t) = \int \frac{d^3k}{(2\pi)^3} f_{\gamma,k}. \tag{A.12}$$

A.2 ALP to two HPs system

Considering the field (for simplicity, we will drop the "" notation to identify the HP in this analysis) to be linearly polarized, we can express it in the following form

$$\vec{A}(\vec{x},t) = \int \frac{d^3k}{(2\pi)^3}\frac{1}{\sqrt{2\omega_k}}\sum_{\lambda=+,-}\left(a_{k,\lambda}(t)\hat{\varepsilon}_{k,\lambda}e^{-i(\omega_k t - \vec{k}\cdot\vec{x})} + a^\dagger_{k,\lambda}(t)\hat{\varepsilon}^*_{k,\lambda}e^{i(\omega_k t - \vec{k}\cdot\vec{x})}\right), \tag{A.13}$$

where $\varepsilon_{k,\hat{\lambda}=\pm}$ and $[a_{k,\lambda(t)}, a^\dagger_{k',\lambda}(t)] = (2\pi)^3\delta^3(k-k')$. Additionally, the basis satisfies the convention

$$\vec{k}\times\hat{\varepsilon}_{k,\lambda} = -i\lambda k\hat{\varepsilon}_{k,\lambda}. \tag{A.14}$$

Also, since the ALP background consists of an oscillatory field, we can express it as

$$\phi(t) = \frac{\phi_0}{2}\left[e^{im_\phi t} + e^{-im_\phi t}\right]. \tag{A.15}$$

Replacing these relations into Eqs. (4.22) and (4.23) we obtain

$$\begin{aligned}&\left(-2i\omega_k\dot{a}_{k,\lambda}\hat{\varepsilon}_{k,\lambda}e^{-i(\omega_k t-\vec{k}\cdot\vec{x})} + 2i\omega_k\dot{a}^\dagger_{k,\lambda}\hat{\varepsilon}^*_{k,\lambda}e^{i(\omega_k t-\vec{k}\cdot\vec{x})}\right)\\ &\quad= \frac{g_{\phi\gamma'\gamma'}\phi_0 m_\phi}{2}(e^{im_\phi t} - e^{-im_\phi t})\left(a_{k,\lambda}(\vec{k}\times\hat{\varepsilon}_{k,\lambda})e^{-i(\omega_k t-\vec{k}\cdot\vec{x})} + a^\dagger_{k,\lambda}(\vec{k}\times\hat{\varepsilon}^*_{k,\lambda})e^{i(\omega_k t-\vec{k}\cdot\vec{x})}\right).\end{aligned} \tag{A.16}$$

where we have neglected the second derivative terms on the amplitudes since we consider them to vary much more slowly than $e^{\pm i\omega_k t}$, also, it is important to mention that we have a sum over $\lambda = \pm$. Let us first consider the equation for $a_{k,+}$ which is given by

$$\partial_t a_{k,\lambda} = \frac{g_{\phi\gamma'\gamma'}\phi_0 m_\phi}{4}\left[a_{k,\lambda}e^{im_\phi t} - a_{k,\lambda}e^{-im_\phi t} + a^\dagger_{-k,\lambda}e^{-i\kappa t}\right]. \tag{A.17}$$

Once again, as we are interested in the process $\phi \to \gamma' + \gamma'$ we focus on the last term, obtaining the equation

$$\partial_t a_{k,+} = \Omega e^{-i\kappa t}a^\dagger_{-k,+}. \tag{A.18}$$

where we have defined $\Omega = g_{\phi\gamma'\gamma'}m_\phi\phi_0/4$. For completeness, we see that the rest of the equations of the system are given by

$$\partial_t a^\dagger_{-k,+} = \Omega e^{i\kappa t}a_{k,+}, \tag{A.19}$$

$$\partial_t a_{k,-} = -\Omega e^{-i\kappa t}a^\dagger_{-k,-}, \tag{A.20}$$

$$\partial_t a^\dagger_{-k,-} = -\Omega e^{i\kappa t}a_{k,-}. \tag{A.21}$$

The solutions for these differential equations are

$$a_{k,+}(t) = e^{-\frac{i\kappa t}{2}}\left[a_{k,+}(0)(\cosh st + \frac{i\kappa}{2s}\sinh st) + \frac{\Omega}{s}a^\dagger_{-k,+}(0)\sinh st\right], \tag{A.22}$$

$$a^\dagger_{-k,+}(t) = e^{\frac{i\kappa t}{2}}\left[a^\dagger_{-k,+}(0)(\cosh st - \frac{i\kappa}{2s}\sinh st) + \frac{\Omega}{s}a_{k,+}(0)\sinh st\right], \tag{A.23}$$

$$a_{k,-}(t) = e^{-\frac{i\kappa t}{2}}\left[a_{k,-}(0)(\cosh st + \frac{i\kappa}{2s}\sinh st) - \frac{\Omega}{s}a^\dagger_{-k,-}(0)\sinh st\right], \tag{A.24}$$

$$a^\dagger_{-k,-}(t) = e^{\frac{i\kappa t}{2}}\left[a^\dagger_{-k,-}(0)(\cosh st - \frac{i\kappa}{2s}\sinh st) - \frac{\Omega}{s}a_{k,-}(0)\sinh st\right], \tag{A.25}$$

where $s = \frac{1}{2}\sqrt{4\Omega^2 - \kappa^2}$. We can then define the number operator $N_+ = a^\dagger_{k,+}a_{k,+}$ and we can obtain the initial occupation number density from

$$f_{+\gamma,k}(t) = \frac{1}{V}\langle i|\, N_+ \,|i\rangle, \tag{A.26}$$

$$f_{-\gamma,k}(t) = \frac{1}{V}\langle i|\, N_- \,|i\rangle, \tag{A.27}$$

which after replacing the solutions for $a_{k,+}$ and $a^\dagger_{k,+}$ gives us for the "+" polarization

$$f_{+\gamma',k}(t) = f_{+\gamma',k}(0)\left(\cosh^2(st) + \frac{\kappa^2}{4s^2}\sinh^2(st)\right) + f_{+\gamma',-k}(0)\frac{\Omega_k^2}{s^2}\sinh^2(st) + \frac{\Omega_k^2}{s^2}\sinh^2(st). \tag{A.28}$$

Then the number density of HP produced by the decay process is found to be

$$n_{+\gamma'} = \int \frac{d^3k}{(2\pi)^3} f_{+\gamma',k}, \tag{A.29}$$

which considering no initial HP of either polarization, gives us the number density of the simple form

$$n_{+\gamma'} = \int \frac{d^3k}{(2\pi)^3} \frac{\Omega^2}{s^2} \sinh^2 st. \tag{A.30}$$

Appendix B

Parametric Resonance

Parametric resonance is a phenomenon that can be observed in a driven harmonic oscillatory movement. It consists in a simple harmonic oscillator that is under a small external effect of a periodic force proportional to the position. We can look at it in the simple form

$$\ddot{x} + \omega_0^2 x = -x f(t) \tag{B.1}$$

where we consider $f(t)$ to be the external force responsible for the driven motion. As a first approximation, for $f(t) = 0$ we simply have a harmonic oscillator, whose solution is well-known to be

$$x_0(t) = A\cos\omega_0 t + B\sin\omega_0 t. \tag{B.2}$$

As we mentioned before, we require the perturbations of the simple harmonic oscillator to be periodic and small, so we can consider them to be of the form

$$f(t) = \omega_0^2 h\cos(\omega t) \tag{B.3}$$

where $h \ll 1$ and the term ω_0^2 is put for convenience. Eq. (B.1) is then

$$\ddot{x} + \omega_0^2 x = -\omega_0^2 h\cos(\omega t)x \tag{B.4}$$

which is called Mathieu's equation. Considering the solution for Eq. (B.4) to be a variation of Eq. (B.2), we can replace it to obtain in the R.H.S., using trigonometric identities, the following terms

$$\cos(\omega t)\cos(\omega_0 t) = \frac{1}{2}\left[\cos((\omega+\omega_0)t) + \cos((\omega-\omega_0)t)\right], \tag{B.5}$$

$$\cos(\omega t)\sin(\omega_0 t) = \frac{1}{2}[\sin((\omega+\omega_0)t) - \sin((\omega-\omega_0)t)]. \tag{B.6}$$

Here we see that if $\omega = 2\omega_0$ the last term in both equations gives a resonant term, i.e., a term with the same frequency as the unperturbed solution, giving us the point of maximal resonance effect. Parametric resonance also allows us to consider a resonance interval, which consists in a window around a maximal resonance point, where we still observe the solution to have increasing amplitudes. To find this interval

of resonance, let us define $\rho = \omega_0 + \epsilon/2$, where $\epsilon \ll 1$ is a small deviation from the natural frequency of the system, this allows us now to consider the ansatz for the general solution to be

$$x(t) = A(t)\cos(\rho t) + B(t)\sin(\rho t), \tag{B.7}$$

where the amplitudes vary slowly in time. Replacing this ansatz in Eq.(B.4) and neglecting the second-order terms of ϵ as well as the second derivative term of the amplitudes, we obtain the resonant terms to be

$$\left[2\dot{A} + \left(\epsilon + \frac{1}{2}\omega_0 h\right) B\right]\sin(\rho t) + \left[2\dot{B} + \left(-\epsilon + \frac{1}{2}\omega_0 h\right) A\right]\cos(\rho t) = 0, \tag{B.8}$$

which, if we consider the amplitudes to be slowly varying in time, they can be expressed as $\{A, B\} = \{A_0, B_0\}e^{st}$, then it gives us a system of equations for the amplitudes $\{A(t), B(t)\}$ of the form

$$\begin{array}{rcl} 2sA_0 + \left(\epsilon + \frac{1}{2}h\omega_0\right) B_0 & = & 0, \\ 2sB_0 + \left(-\epsilon + \frac{1}{2}h\omega_0\right) A_0 & = & 0. \end{array} \tag{B.9}$$

Considering non-trivial solutions, this gives us a clear condition between the parameters of the system if we want the solutions that increase exponentially in time, this is

$$s = \pm\frac{1}{2}\sqrt{\left(\frac{h\omega_0}{2}\right)^2 - \epsilon^2} \longrightarrow -\frac{h\omega_0}{2} < \epsilon < \frac{h\omega_0}{2}. \tag{B.10}$$

Generally, $\mu = 2s$ is called the Floquet exponent, and it is used in several studies regarding Floquet theory. The general solution with an increasing amplitude due to parametric resonance effects is then given by

$$x(t) = e^{\frac{t}{2}\sqrt{\left(\frac{h\omega_0}{2}\right)^2 - \epsilon^2}}(a_0\cos((\omega_0 + \epsilon/2)t) + b_0\sin((\omega_0 + \epsilon/2)t)). \tag{B.11}$$

where we have only considered the positive exponent for the solution since we are interested in the solutions with increasing amplitudes.

We need now to implement these features in the models studied. The most important result of this analysis is the interval of resonance. Taking into consideration the system of an ALP decaying to two HPs, the energy conservation coincides with the requirement $\omega_0 = \omega/2$, which in the system is given by $m_\phi = 2\omega$, where m_ϕ is the ALP mass (background frequency) and ω in the HP frequency (unperturbed system). Looking at the Floquet exponent, we express the solution as hyperbolic functions, but the factor s remains the same for both this general analysis and for the physical model studied, we see then that its form, given by $s = \frac{1}{2}\sqrt{4\Omega_k^2 - \kappa^2}$ can be related to the expression found, $s = \frac{1}{2}\sqrt{(\frac{h\omega_0}{2})^2 - \epsilon^2}$ so we can identify the relation $(\frac{h\omega_0}{2}) \to 2\Omega_k$ and $\epsilon \to \kappa$. Finally, the resonance window is found to be, in terms of the parameters of the system, given by

$$-2\Omega_k < \kappa < 2\Omega_k, \tag{B.12}$$

this allows us to identify the resonance window for the system since $\epsilon \to \kappa$ and ϵ is related to the resonance window, we obtain in the system that the maximum value of momentum dispersion corresponds to $2\Omega_k$,

and we can then say the condition for resonance in this analysis, coincides with the condition for $s^2 > 0$. This then allows us to relate the resonance window with the dispersion of the momentum caused by the expansion of the universe, which is a very useful tool to rapidly identify the space parameter that indicates resonance and the time while it is present in each system.

References

[1] Rouzbeh Allahverdi et al. "The First Three Seconds: a Review of Possible Expansion Histories of the Early Universe". In: *The Open Journal of Astrophysics* 4.1 (Jan. 2021). DOI: 10.21105/astro.2006.16182. URL: https://doi.org/10.21105%2Fastro.2006.16182.

[2] George R. Blumenthal et al. "Formation of Galaxies and Large Scale Structure with Cold Dark Matter". In: *Nature* 311 (1984). Ed. by M. A. Srednicki, pp. 517–525. DOI: 10.1038/311517a0.

[3] N. Aghanim et al. "Planck 2018 results". In: *Astronomy & Astrophysics* 641 (Oct. 2020). ISSN: 1432-0746. DOI: 10.1051/0004-6361/201833910. URL: http://dx.doi.org/10.1051/0004-6361/201833910.

[4] Vera C. Rubin and Jr. Ford W. Kent. "Rotation of the Andromeda Nebula from a Spectroscopic Survey of Emission Regions". In: 159 (Feb. 1970), p. 379. DOI: 10.1086/150317.

[5] Yoshiaki Sofue and Vera Rubin. "Rotation Curves of Spiral Galaxies". In: *Annual Review of Astronomy and Astrophysics* 39.1 (Sept. 2001), pp. 137–174. DOI: 10.1146/annurev.astro.39.1.137. URL: https://doi.org/10.1146%5C%2Fannurev.astro.39.1.137.

[6] Katherine Freese. "Status of dark matter in the universe". In: *International Journal of Modern Physics D* 26.06 (Mar. 2017), p. 1730012. DOI: 10.1142/s0218271817300129. URL: https://doi.org/10.1142%2Fs0218271817300129.

[7] N. W. Halverson et al. "Degree Angular Scale Interferometer First Results: A Measurement of the Cosmic Microwave Background Angular Power Spectrum". In: *The Astrophysical Journal* 568.1 (Mar. 2002), p. 38. DOI: 10.1086/338879. URL: https://dx.doi.org/10.1086/338879.

[8] Eleonora Di Valentino. "Challenges of the Standard Cosmological Model". In: *Universe* 8.8 (2022). ISSN: 2218-1997. DOI: 10.3390/universe8080399. URL: https://www.mdpi.com/2218-1997/8/8/399.

[9] Jian-Ping Hu and Fa-Yin Wang. "Hubble Tension: The Evidence of New Physics". In: *Universe* 9.2 (2023). ISSN: 2218-1997. DOI: 10.3390/universe9020094. URL: https://www.mdpi.com/2218-1997/9/2/94.

[10] Moira Venegas. *Relic Density of Axion Dark Matter in Standard and Non-Standard Cosmological Scenarios*. 2021. DOI: 10.48550/ARXIV.2106.07796. URL: https://arxiv.org/abs/2106.07796.

[11] Keith A. Olive. *Primordial Nucleosynthesis*. 1996. DOI: 10.48550/ARXIV.ASTRO-PH/9609071. URL: https://arxiv.org/abs/astro-ph/9609071.

[12] Brian D. Fields et al. "Model independent predictions of big bang nucleosynthesis from He and Li: consistency and implications". In: *New Astronomy* 1.1 (July 1996), pp. 77–96. DOI: 10.1016/s1384-1076(96)00007-3. URL: https://doi.org/10.1016%5C%2Fs1384-1076%5C%2896%5C%2900007-3.

[13] Katherine Freese, Brian Fields, and David Graff. "Death of Stellar Baryonic Dark Matter". In: *ESO ASTROPHYSICS SYMPOSIA*. Springer Berlin Heidelberg, Sept. 2003, pp. 18–23. DOI: 10.1007/10719504_3. URL: https://doi.org/10.1007%2F10719504_3.

[14] Hans Peter Nilles. "Supersymmetry, Supergravity and Particle Physics". In: *Phys. Rept.* 110 (1984), pp. 1–162. DOI: 10.1016/0370-1573(84)90008-5.

[15] Géraldine Servant and Tim M.P. Tait. "Is the lightest Kaluza–Klein particle a viable dark matter candidate?" In: *Nuclear Physics B* 650.1-2 (Feb. 2003), pp. 391–419. DOI: 10.1016/s0550-3213(02)01012-x. URL: https://doi.org/10.1016%5C%2Fs0550-3213%5C%2802%5C%2901012-x.

[16] Chuan-Ren Chen, Ming-Che Lee, and Ho-Chin Tsai. "Implications of the Little Higgs Dark Matter and T-odd fermions". In: *Journal of High Energy Physics* 2014.6 (2014), pp. 1–16.

[17] Leszek Roszkowski. "Particle dark matter: A Theorist's perspective". In: *Pramana* 62 (2004). Ed. by D. P. Roy, S. Banerjee, and K. Sridhar, pp. 389–401. DOI: 10.1007/BF02705097. arXiv: hep-ph/0404052.

[18] Joerg Jaeckel. *A force beyond the Standard Model - Status of the quest for hidden photons*. 2013. DOI: 10.48550/ARXIV.1303.1821. URL: https://arxiv.org/abs/1303.1821.

[19] Andrew J. Long and Lian-Tao Wang. "Dark photon dark matter from a network of cosmic strings". In: *Physical Review D* 99.6 (Mar. 2019). DOI: 10.1103/physrevd.99.063529. URL: https://doi.org/10.1103%5C%2Fphysrevd.99.063529.

[20] Paola Arias et al. "Hidden photon dark matter interacting via axion-like particles". In: *Journal of Cosmology and Astroparticle Physics* 2021.05 (May 2021), p. 070. DOI: 10.1088/1475-7516/2021/05/070. URL: https://doi.org/10.1088%5C%2F1475-7516%5C%2F2021%5C%2F05%5C%2F070.

[21] R. D. Peccei and Helen R. Quinn. "CP Conservation in the Presence of Pseudoparticles". In: *Phys. Rev. Lett.* 38 (25 June 1977), pp. 1440–1443. DOI: 10.1103/PhysRevLett.38.1440. URL: https://link.aps.org/doi/10.1103/PhysRevLett.38.1440.

[22] Steven Weinberg. "A New Light Boson?" In: *Phys. Rev. Lett.* 40 (4 Jan. 1978), pp. 223–226. DOI: 10.1103/PhysRevLett.40.223. URL: https://link.aps.org/doi/10.1103/PhysRevLett.40.223.

[23] Peter Graf and Frank Daniel Steffen. "Thermal axion production in the primordial quark-gluon plasma". In: *Physical Review D* 83.7 (Apr. 2011). DOI: 10.1103/physrevd.83.075011. URL: https://doi.org/10.1103%5C%2Fphysrevd.83.075011.

[24] Michael S. Turner. "Early-Universe Thermal Production of Not-So-Invisible Axions". In: *Phys. Rev. Lett.* 59 (21 Nov. 1987), pp. 2489–2492. DOI: 10.1103/PhysRevLett.59.2489. URL: https://link.aps.org/doi/10.1103/PhysRevLett.59.2489.

[25] K. Saikawa. "Production and evolution of axion dark matter in the early universe". PhD thesis. University of Tokyo, 2013.

[26] T W B Kibble. "Topology of cosmic domains and strings". In: *Journal of Physics A: Mathematical and General* 9.8 (Aug. 1976), p. 1387. DOI: 10.1088/0305-4470/9/8/029. URL: https://dx.doi.org/10.1088/0305-4470/9/8/029.

[27] Mark Hindmarsh, Russell Kirk, and Stephen M. West. "Dark matter from decaying topological defects". In: *Journal of Cosmology and Astroparticle Physics* 2014.03 (Mar. 2014), pp. 037–037. DOI: 10.1088/1475-7516/2014/03/037. URL: https://doi.org/10.1088%5C%2F1475-7516%5C%2F2014%5C%2F03%5C%2F037.

[28] Masahiro Kawasaki, Ken'ichi Saikawa, and Toyokazu Sekiguchi. "Axion dark matter from topological defects". In: *Physical Review D* 91.6 (Mar. 2015). DOI: 10.1103/physrevd.91.065014. URL: https://doi.org/10.1103%5C%2Fphysrevd.91.065014.

[29] R.L. Davis. "Cosmic axions from cosmic strings". In: *Physics Letters B* 180.3 (1986), pp. 225–230. ISSN: 0370-2693. DOI: https://doi.org/10.1016/0370-2693(86)90300-X. URL: https://www.sciencedirect.com/science/article/pii/037026938690300X.

[30] David H. Lyth. "Estimates of the cosmological axion density". In: *Physics Letters B* 275.3 (1992), pp. 279–283. ISSN: 0370-2693. DOI: https://doi.org/10.1016/0370-2693(92)91590-6. URL: https://www.sciencedirect.com/science/article/pii/0370269392915906.

[31] P. Sikivie and Q. Yang. "Bose-Einstein Condensation of Dark Matter Axions". In: *Physical Review Letters* 103.11 (Sept. 2009). DOI: 10.1103/physrevlett.103.111301. URL: https://doi.org/10.1103%5C%2Fphysrevlett.103.111301.

[32] In: 2018 (Nov. 2018). DOI: 10.1088/1475-7516/2018/11/004. URL: https://doi.org/10.1088%5C%2F1475-7516%5C%2F2018%5C%2F11%5C%2F004.

[33] Paola Arias et al. "WISPy cold dark matter". In: *Journal of Cosmology and Astroparticle Physics* 2012.06 (June 2012), pp. 013–013. DOI: 10.1088/1475-7516/2012/06/013. URL: https://doi.org/10.1088%2F1475-7516%2F2012%2F06%2F013.

[34] Andrew J. Long and Lian-Tao Wang. "Dark photon dark matter from a network of cosmic strings". In: *Physical Review D* 99.6 (Mar. 2019). DOI: 10.1103/physrevd.99.063529. URL: https://doi.org/10.1103%5C%2Fphysrevd.99.063529.

[35] Peter W. Graham, Jeremy Mardon, and Surjeet Rajendran. "Vector dark matter from inflationary fluctuations". In: *Physical Review D* 93.10 (May 2016). DOI: 10.1103/physrevd.93.103520. URL: https://doi.org/10.1103%5C%2Fphysrevd.93.103520.

[36] Licia Verde, Tommaso Treu, and Adam G. Riess. "Tensions between the early and late Universe". In: *Nature Astronomy* 3.10 (Sept. 2019), pp. 891–895. DOI: 10.1038/s41550-019-0902-0. URL: https://doi.org/10.1038%5C%2Fs41550-019-0902-0.

[37] Richard A. Battye, Tom Charnock, and Adam Moss. "Tension between the power spectrum of density perturbations measured on large and small scales". In: *Physical Review D* 91.10 (May 2015). DOI: 10.1103/physrevd.91.103508. URL: https://doi.org/10.1103%5C%2Fphysrevd.91.103508.

[38] Alexander Vilenkin and L. H. Ford. "Gravitational effects upon cosmological phase transitions". In: *Phys. Rev. D* 26 (6 Sept. 1982), pp. 1231–1241. DOI: 10.1103/PhysRevD.26.1231. URL: https://link.aps.org/doi/10.1103/PhysRevD.26.1231.

[39] G.D. Coughlan et al. "Cosmological problems for the polonyi potential". In: *Physics Letters B* 131.1 (1983), pp. 59–64. ISSN: 0370-2693. DOI: https://doi.org/10.1016/0370-2693(83)91091-2. URL: https://www.sciencedirect.com/science/article/pii/0370269383910912.

[40] L. H. Ford. "Gravitational particle creation and inflation". In: *Phys. Rev. D* 35 (10 May 1987), pp. 2955–2960. DOI: 10.1103/PhysRevD.35.2955. URL: https://link.aps.org/doi/10.1103/PhysRevD.35.2955.

[41] Boris Spokoiny. "Deflationary Universe scenario". In: *Physics Letters B* 315.1-2 (Sept. 1993), pp. 40–45. DOI: 10.1016/0370-2693(93)90155-b. URL: https://doi.org/10.1016%5C%2F0370-2693%5C%2893%5C%2990155-b.

[42] Daniel J. H. Chung, Edward W. Kolb, and Antonio Riotto. "Production of massive particles during reheating". In: *Physical Review D* 60.6 (Aug. 1999). DOI: 10.1103/physrevd.60.063504. URL: https://doi.org/10.1103%5C%2Fphysrevd.60.063504.

[43] Paola Arias et al. "New opportunities for axion dark matter searches in nonstandard cosmological models". In: *Journal of Cosmology and Astroparticle Physics* 2021.11 (Nov. 2021), p. 003. DOI: 10.1088/1475-7516/2021/11/003. URL: https://doi.org/10.1088%2F1475-7516%2F2021%2F11%2F003.

[44] Daiske Yoshida and Jiro Soda. "Electromagnetic waves propagating in the string axiverse". In: *Progress of Theoretical and Experimental Physics* 2018.4 (Apr. 2018). DOI: 10.1093/ptep/pty029. URL: https://doi.org/10.1093%2Fptep%2Fpty029.

[45] Mark P. Hertzberg and Enrico D. Schiappacasse. "Dark matter axion clump resonance of photons". In: *Journal of Cosmology and Astroparticle Physics* 2018.11 (Nov. 2018), pp. 004–004. DOI: 10.1088/1475-7516/2018/11/004. URL: https://doi.org/10.1088%2F1475-7516%2F2018%2F11%2F004.

[46] Ariel Arza. "Photon enhancement in a homogeneous axion dark matter background". In: *The European Physical Journal C* 79.3 (Mar. 2019). DOI: 10.1140/epjc/s10052-019-6759-7. URL: https://doi.org/10.1140%5C%2Fepjc%5C%2Fs10052-019-6759-7.

[47] Zihang Wang, Lijing Shao, and Li-Xin Li. "Resonant instability of axionic dark matter clumps". In: *Journal of Cosmology and Astroparticle Physics* 2020.07 (July 2020), pp. 038–038. DOI: 10.1088/1475-7516/2020/07/038. URL: https://doi.org/10.1088%5C%2F1475-7516%5C%2F2020%5C%2F07%5C%2F038.

[48] Ariel Arza, Thomas Schwetz, and Elisa Todarello. "How to suppress exponential growth—on the parametric resonance of photons in an axion background". In: *Journal of Cosmology and Astroparticle Physics* 2020.10 (Oct. 2020), pp. 013–013. DOI: 10.1088/1475-7516/2020/10/013. URL: https://doi.org/10.1088%5C%2F1475-7516%5C%2F2020%5C%2F10%5C%2F013.

[49] Gonzalo Alonso-Álvarez et al. "On the wondrous stability of ALP dark matter". In: *Journal of Cosmology and Astroparticle Physics* 2020.03 (Mar. 2020), pp. 052–052. DOI: 10.1088/1475-7516/2020/03/052. URL: https://doi.org/10.1088%2F1475-7516%2F2020%2F03%2F052.

[50] Javier Redondo and Marieke Postma. "Massive hidden photons as lukewarm dark matter". In: *Journal of Cosmology and Astroparticle Physics* 2009.02 (Feb. 2009), pp. 005–005. DOI: 10.1088/1475-7516/2009/02/005. URL: https://doi.org/10.1088%5C%2F1475-7516%5C%2F2009%5C%2F02%5C%2F005.

[51] Ariel Arza. *Production of massive bosons from the decay of a massless particle beam*. 2022. arXiv: 2009.03870 [hep-th].

[52] Joerg Jaeckel and Sebastian Schenk. "Challenging the stability of light millicharged dark matter". In: *Physical Review D* 103.10 (May 2021). DOI: 10.1103/physrevd.103.103523. URL: https://doi.org/10.1103%5C%2Fphysrevd.103.103523.

[53] Lev Kofman, Andrei, and Alexei A. Starobinsky. "Reheating after Inflation". In: *Physical Review Letters* 73.24 (Dec. 1994), pp. 3195–3198. DOI: 10.1103/physrevlett.73.3195. URL: https://doi.org/10.1103%5C%2Fphysrevlett.73.3195.

[54] Lev Kofman, Andrei Linde, and Alexei A. Starobinsky. "Towards the theory of reheating after inflation". In: *Physical Review D* 56.6 (Sept. 1997), pp. 3258–3295. DOI: 10.1103/physrevd.56.3258. URL: https://doi.org/10.1103%5C%2Fphysrevd.56.3258.

[55] J F Dufaux et al. "Preheating with trilinear interactions: tachyonic resonance". In: *Journal of Cosmology and Astroparticle Physics* 2006.07 (July 2006), pp. 006–006. DOI: 10.1088/1475-7516/2006/07/006. URL: https://doi.org/10.1088%5C%2F1475-7516%5C%2F2006%5C%2F07%5C%2F006.

[56] Jeff A. Dror, Keisuke Harigaya, and Vijay Narayan. "Parametric resonance production of ultralight vector dark matter". In: *Phys. Rev. D* 99 (3 Feb. 2019), p. 035036. DOI: 10.1103/PhysRevD.99.035036. URL: https://link.aps.org/doi/10.1103/PhysRevD.99.035036.